tGolgin-1 (p230, golgin-245) modulates Shiga-toxin transport to the Golgi and Golgi motility towards the microtubule-organizing centre

Atsuko Yoshino[1], Subba Rao Gangi Setty[1], Clare Poynton[2], Eileen L. Whiteman[3], Agnès Saint-Pol[4], Christopher G. Burd[5], Ludger Johannes[4], Erika L. Holzbaur[6], Michael Koval[6], J. Michael McCaffery[2] and Michael S. Marks[1,*]

[1]Department of Pathology and Laboratory Medicine, [3]Department of Medicine, [5]Department of Cell and Developmental Biology, [6]Department of Physiology, University of Pennsylvania School of Medicine, Philadelphia, PA 19104-6082, USA
[2]Integrated Imaging Center, Department of Biology, Johns Hopkins University, Baltimore, MD 21218, USA
[4]Institut Curie, CNRS-UMR144, F-75248 Paris, Cedex 75005, France
*Author for correspondence (e-mail: marksm@mail.med.upenn.edu)

Accepted 2 March 2005
Journal of Cell Science 118, 2279-2293 Published by The Company of Biologists 2005
doi:10.1242/jcs.02358

Summary

tGolgin-1 (trans-Golgi p230, golgin-245) is a member of a family of large peripheral membrane proteins that associate with the trans-Golgi network (TGN) via a C-terminal GRIP domain. Some GRIP-domain proteins have been implicated in endosome-to-TGN transport but no function for tGolgin-1 has been described. Here, we show that tGolgin-1 production is required for efficient retrograde distribution of Shiga toxin from endosomes to the Golgi. Surprisingly, we also found an indirect requirement for tGolgin-1 in Golgi positioning. In HeLa cells depleted of tGolgin-1, the normally centralized Golgi and TGN membranes were displaced to the periphery, forming 'mini stacks'. These stacks resembled those in cells with disrupted microtubules or dynein-dynactin motor, in that they localized to endoplasmic-reticulum exit sites, maintained their secretory capacity and cis-trans polarity, and were relatively immobile by video microscopy. The mini stacks formed concomitant with a failure of pre-Golgi elements to migrate along microtubules towards the microtubule-organizing centre. The requirement for tGolgin-1 in Golgi positioning did not appear to reflect direct binding of tGolgin-1 to motile pre-Golgi membranes, because distinct Golgi and tGolgin-1-containing TGN elements that formed after recovery of HeLa cells from brefeldin-A treatment moved independently toward the microtubule-organizing centre. These data demonstrate that tGolgin-1 functions in Golgi positioning indirectly, probably by regulating retrograde movement of cargo required for recruitment or activation of dynein-dynactin complexes on newly formed Golgi elements.

Supplementary material available online at
http://jcs.biologists.org/cgi/content/full/118/10/2279/DC1

Key words: Dynein, Dynactin, Centrosome, Retrograde transport, Endosome

Introduction

The Golgi complex plays a central role in glycoprotein processing and quality control of secretion in eukaryotic cells. The vertebrate Golgi complex consists, during interphase, of polarized, stacked cisternae that appose the microtubule-organizing centre (MTOC). This central positioning might facilitate concentration of secretory cargo during transport from the endoplasmic reticulum (ER) through the Golgi stacks and trans-Golgi network (TGN) to post-Golgi compartments, as well as polarized secretion to establish cellular polarity, migration and other effector functions (Rios and Bornens, 2003; Warren and Shorter, 2002). Golgi positioning at the MTOC requires the integrity of microtubules (Ho et al., 1989; Rogalski and Singer, 1984) and the minus-end-directed dynein-dynactin microtubule motor complex (Burkhardt et al., 1997; Corthesy-Theulaz et al., 1992; Harada et al., 1998). Tubulovesicular clusters that emerge near exit sites from the ER recruit dynein-dynactin complexes and migrate towards the MTOC along microtubules (Burkhardt et al., 1997; Cole et al., 1996a; Corthesy-Theulaz et al., 1992; Ho et al., 1989; Presley et al., 1997; Storrie et al., 1998). Several factors have been implicated in both the recruitment of dynein-dynactin motors to pre-Golgi elements (Holleran et al., 2001; Muresan et al., 2001; Matanis et al., 2002; Short et al., 2002) and the consequent tethering of newly formed cis-Golgi membranes at the MTOC (Ladinsky et al., 1999; Marsh et al., 2001; Gillingham et al., 2004; Infante et al., 1999; Pernet-Gallay et al., 2002; Rios et al., 2004; Takahashi et al., 1999; Walenta et al., 2001), but it is not known how the localization and activity of these and other potential recruitment and tethering factors are regulated. One challenge for the cell is to maintain a steady-state distribution of these factors in the face of a massive flow of membrane transport into and out of the Golgi complex (Rios and Bornens, 2003). One way to accomplish this distribution is to recycle recruitment factors from pre- and/or post-Golgi compartments.

As part of an effort to understand membrane dynamics at the TGN, we have been studying members of a group of peripheral

TGN membrane proteins, referred to here as GRIP proteins, characterized by extensive predicted coiled-coil structure and a C-terminal GRIP (golgin-97, RanBP1, Imh1p, p230) domain (Barr, 1999; Kjer-Nielsen et al., 1999a; Munro and Nichols, 1999). Two mammalian GRIP proteins, tGolgin-1 (also known as golgin-245 and trans-Golgi p230; gene name, *golga4*) (Cowan et al., 2002; Erlich et al., 1996; Fritzler et al., 1995) and golgin-97 (gene name, *golga1*) (Griffith et al., 1997), were identified as autoantigens in patients with Sjögren's syndrome. Two others, GCC88 and GCC185 (Luke et al., 2003), were identified by sequence homology and appear to be functionally unrelated (Derby et al., 2004). The GRIP domains of tGolgin-1 and golgin-97 mediate localization to the cytoplasmic face of the TGN via interaction with the small GTPase Arl1 (Lu and Hong, 2003; Panic et al., 2003a; Panic et al., 2003b; Setty et al., 2003; Wu et al., 2004). Although modest production of these isolated GRIP domains results in the displacement of endogenous golgin-97 and tGolgin-1 from the TGN (Kjer-Nielsen et al., 1999a; Kjer-Nielsen et al., 1999b), probably by competition for limiting Arl1-GTP, overproduction of these GRIP domains further results in extensive morphological disruption of the TGN concomitant with an inhibition of retrograde transport of TGN-resident proteins from endosomes (Yoshino et al., 2003). This result suggested that tGolgin-1, golgin-97 and/or other Arl1 effectors function in regulating vesicular transport from endosomes to the TGN, a notion supported by genetic analyses of the single GRIP protein Imh1p in yeast (Li and Warner, 1996; Siniossoglou et al., 2000; Tsukada et al., 1999) and recently demonstrated for mammalian golgin-97 (Lu et al., 2004). To test whether tGolgin-1 shares a similar function, we assessed the consequences of reduced tGolgin-1 production in HeLa cells. Our results are consistent with a role for tGolgin-1 in regulating retrograde transport of Shiga toxin to the Golgi. More surprisingly, however, our results demonstrate a critical requirement for tGolgin-1 production in the minus-end-directed transport of Golgi elements along microtubules. Based on our data and the reported Golgi fragmentation observed upon disruption of other proteins required for retrograde transport (Lu et al., 2004; Seaman, 2004), we propose that recruitment of microtubule motors to the Golgi requires tGolgin-1-dependent retrograde transport from endosomes.

Materials and Methods

Antibodies

To generate a rabbit polyclonal antiserum to tGolgin-1, we produced in *Escherichia coli* (strain BL21[DE3]) a fragment corresponding to the first 624 residues of mouse tGolgin-1, with a C-terminal six-histidine-residue tag. Soluble fusion protein was purified from sonicated bacteria using His-bind resin (Novagen, San Diego, CA) according to the manufacturer's instructions. Following fractionation by SDS-PAGE, a band corresponding to the 72,500 M_r predicted fusion protein was excised and injected i.d. into rabbits at 2- to 3-week intervals by Cocalico Biologicals (Reamstown, PA). Sera collected 10 days after the last injection specifically recognize both human and mouse tGolgin-1.

The following antibodies against the indicated proteins were obtained from the sources listed: sheep anti-TGN46, Serotec, Oxford, UK; rabbit

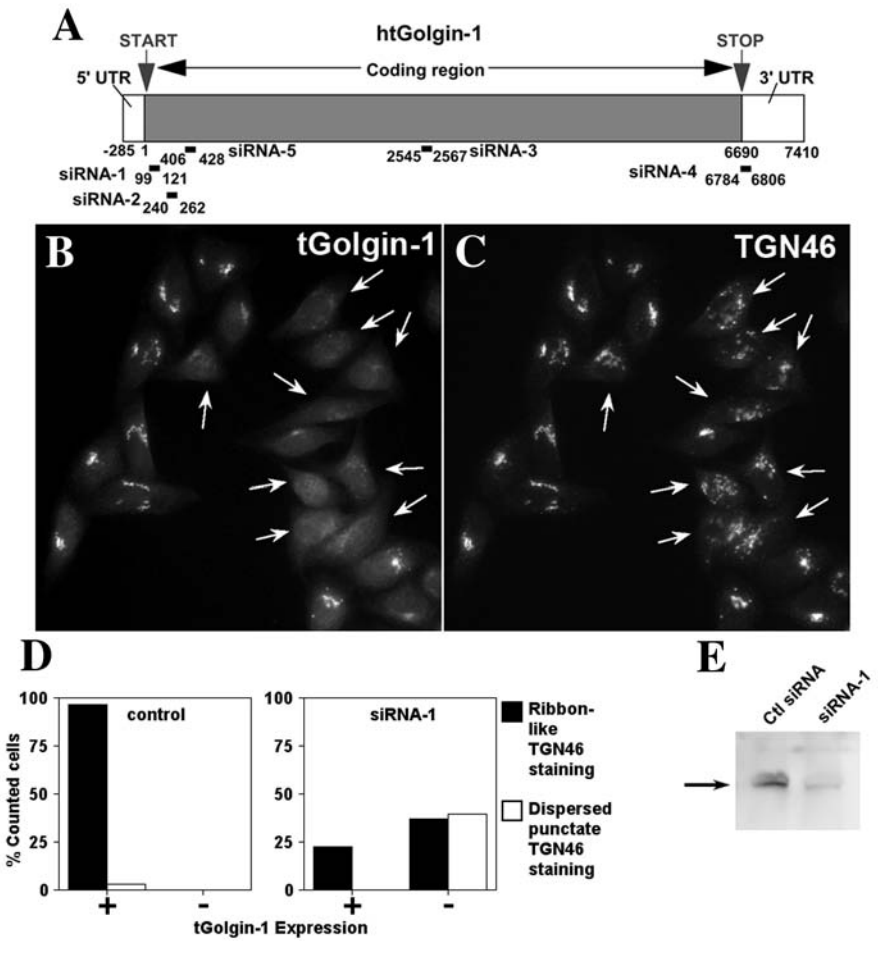

Fig. 1. Depletion of tGolgin-1 from HeLa cells using siRNA. (A) The mRNA encoding tGolgin-1, showing the positions of the overlapping 21-mers used for siRNAs relative to the coding region and the 5′ and 3′ untranslated regions. See Table 1 for the sequences of the oligonucleotides. (B,C) Low-magnification (40×) IFM image of tGolgin-1 (B) and TGN46 (C) expression in HeLa cells transduced once 2 days earlier with siRNA-1. Cells were co-stained with antibodies against tGolgin-1 and TGN46, and with appropriate fluorochrome-conjugated secondary antibodies. Arrows denote cells with reduced tGolgin-1 expression. (D) Untransfected HeLa cells (control) or cells transduced once with siRNA-1 were analysed by IFM as in B,C. Cells were counted as positive or negative for tGolgin-1 expression as indicated and, within each population, cells were scored for a 'normal' ribbon-like or a dispersed, punctate staining pattern for TGN46 in single plane images. The proportions of cells in each category are given from a representative experiment. Results with two control siRNAs and with siRNA-4 were similar to those obtained with untransfected cells (E). Whole-cell lysates from HeLa cells transduced twice with siRNA-1 or control siRNA were fractionated by SDS-PAGE and analysed by western blot for tGolgin-1 production. Only the portion of the gel corresponding to full-length tGolgin-1 (260 kDa) is shown; the rest of the lanes were blank.

anti-golgin-97 and monoclonal antibody (mAb) anti-golgin-97, E. K. L. Chan (Scripps Research Institute, La Jolla, CA) (Griffith et al., 1997); mAb anti-giantin, H.-P. Hauri (University of Basel, Switzerland) (Linstedt and Hauri, 1993); rabbit anti-β-1,4-galactosyl transferase (GalT), E. Berger (University of Zurich, Switzerland) (Berger and Hesford, 1985); mAb anti-Lamp1 (H4A3), Developmental Studies Hybridoma Bank, Iowa City, IA; anti-CD63 (mAb against CD63), Beckman Coulter, Fullerton, CA; anti-tubulin (mAb YL1/2), Accurate Chemical, Westbury, NY; anti-transferrin receptor (mAb B3/25), Roche Molecular Biochemicals, Indianapolis, IN. mAbs against human tGolgin-1 (p230), EEA1, GM130, p115 and GS28 were from Becton Dickinson/Pharmingen (San Diego, CA). mAbs against acetylated tubulin, γ-tubulin and α-tubulin were from Sigma (St Louis, MO). Secondary antibodies against mouse, rabbit, sheep or rat IgG and conjugated to rhodamine red X (RRX), fluorescein isothiocyanate (FITC) or aminomethylcoumarin acetate (AMCA) were from Jackson ImmunoResearch (West Grove, PA).

Small interfering RNAs and plasmids

21-nucleotide RNA duplexes with symmetric 2-nucleotide 3′-(2′-deoxy)thymidine overhangs were synthesized by Dharmacon (Lafayette, CO) and annealed as described (Elbashir et al., 2001). Small interfering RNAs (siRNAs) 1 to 5 targeting tGolgin-1 were designed as described in Fig. 1A and Table 1, and the control siRNA corresponds to nucleotides 97-115 of the golgin-97 RNA coding sequence; the latter had no effect in multiple experiments on golgin-97 production levels. Plasmids encoding various fusions to enhanced green fluorescent protein (EGFP) have been described: Sec13-EGFP in pBK-CMV (gift from B. Glick, University of Chicago, Chicago, IL) (Hammond and Glick, 2000); GRASP65-EGFP in pEGFP-N2 (gift from M. Lowe, University of Manchester, UK) (Lane et al., 2002); and GalT-EGFP in pSX (Cole et al., 1996b) and the vesicular stomatitis virus glycoprotein fused to EGFP (VSV-G/EGFP) in pCDM8.1 (Presley et al., 1997) (gifts of J. Lippincott-Schwartz, US National Institutes of Health, Bethesda, MD). C-Terminally FLAG-tagged dynamitin in pcDNA3 will be described elsewhere (E.L.H., unpublished). Mouse tGolgin-1, cloned in the *Sal*I-*Xba*I sites of pCDM8.1 (Bonifacino et al., 1990), was constructed from cDNAs previously described (Cowan et al., 2002) and a 5′ *Sal*I-*Bsp*E1 fragment generated by amplification of the cDNA using a primer designed to insert a Kozak consensus start site and codons for the N-terminal five amino acids. HA-Rab27a, subcloned into the *Sal*I-*Xba*I sites of pCDM8.1, was generated by reverse transcription PCR (RT-PCR) from human *MNT-1* melanoma mRNA using primers designed to insert a Kozak consensus start site and a single haemagglutinin (HA) epitope tag at the N-terminus. All newly generated plasmids were sequence verified.

Cell culture and transfection

HeLa cells were maintained in Dulbecco's modified Eagle's medium with 10% foetal bovine serum (FBS). For siRNA transduction, 0.75×10^5 to 3×10^5 HeLa cells per well were plated in 12-well plates in fresh medium without antibiotics. Cells were transduced on day 2 with 1.68 μg siRNA using Oligofectamine (Invitrogen, Carlsbad, CA) according to the manufacturer's instructions. In most experiments, the transfection was repeated 24 hours later, cells were replated onto coverslips the next day, then fixed 1 day later and analysed. Co-transfection of plasmid DNA (0.5-2 μg per well) and siRNA (0.84 μg per well) was done using Lipofectamine 2000 (Invitrogen) according to the manufacturer's instructions in a single transfection. Cells were replated on coverslips the next day and fixed 2 days after transfection. Transfection of plasmids was done in six-well dishes using calcium-phosphate precipitation (Marks et al., 1996) with 7.0-7.5 μg total DNA or in 12-well dishes using Lipofectamine 2000 (Santini et al., 1998) with 2 μg total DNA, and cells were analysed 2 days after transfection. HeLa cells stably producing GRASP65-EGFP (HeLa-GRASP65-EGFP) were prepared by transfection using calcium-phosphate precipitation and selection in 0.8 mg ml^{-1} geneticin (G418). G418-resistant cells were segregated and screened for GFP production by flow cytometry using a FACStar Plus cell sorter (BD Biosciences, San Jose, CA), cloned by limiting dilution and screened for GRASP65-EGFP Golgi localization by fluorescence microscopy.

Nocodazole treatment

To depolymerize microtubules, HeLa cells were incubated on ice for 15 minutes and then treated with 5 μg ml^{-1} nocodazole (Sigma) in DMEM containing 25 mM HEPES, pH 7.4, 10% FBS at 37°C for 2 hours, followed by fixation. Staining with anti-α-tubulin antibodies showed only a diffuse cytoplasmic stain by immunofluorescence microscopy (IFM).

Brefeldin-A washout at 16°C

HeLa cells were incubated with 1 μg ml^{-1} brefeldin A in DMEM containing 10% FBS for 1 hour, washed twice with PBS, incubated with DMEM containing 10% FBS, 25 mM HEPES, pH 7.4, at 16°C for 3 hours and then incubated at 37°C as indicated. At the end of each time period, cells were fixed and analysed by fluorescence microscopy.

Internalization and post-endocytic transport of Shiga-toxin B fragment

HeLa cells were incubated on ice for 45 minutes with Alexa-488-conjugated Shiga-toxin B fragment (STxB, 1:100 dilution of

Table 1. Sequences of siRNA oligonucleotides

siRNA		Sequence	Position in cDNA*
siRNA-1	(sense)	5′-GAAUGAGGAGCAGGACAUCTdT	tg p230
	(antisense)	5′-GAUGUCCUGCUCCUCAUUCdTdT	nt 99-121
siRNA-2	(sense)	5′-AGGAAUCUCUAUUCCGGUCdTdT	tg p230
	(antisense)	5′-GACCGGAAUAGAGAUUCCUdTdT	nt 240-262
siRNA-3	(sense)	5′-GAAAGAUGUUUGUACUGAGdTdT	tg p230
	(antisense)	5′-CUCAGUACAAACAUCUUUCdTdT	nt 2545-2567
siRNA-4	(sense)	5′-CUGUCCACACUUGCUACUCdTdT	tg p230
	(antisense)	5′-GAGUAGCAAGUGUGGACAGdTdT	nt 6784-6806
siRNA-5	(sense)	5′-AGAACAGUUGAUUCAGCGGdTdT	tg p230
	(antisense)	5′-CCGCUGAAUCAACUGUUCUdTdT	nt 406-428
control siRNA	(sense)	5′-UCAGUUGCCUCAAUGGGAGdTdT	golgin-97
	(antisense)	5′-CUCCCAUUGAGGCAACUGAdTdT	nt 97-115

*Positions are relative to the start of the coding sequence predicted from GenBank entries NM_002078 for human *Golga4*/ trans-Golgi p230 and NM_002077 for human *Golga1*/golgin-97.

concentrated stock). Cells were washed with PBS, chased at 37°C for 60 minutes and then fixed and analysed by fluorescence microscopy. Some cells were pretreated on ice for 15 minutes and 37°C for 2 hours with nocodazole (5 μg ml^{-1}) before STxB incorporation in the presence of nocodazole (1 μg ml^{-1}). Cells transduced with siRNA were used 3 days after the first transfection.

Immunofluorescence microscopy

HeLa cells were fixed with either 2% formaldehyde for 25 minutes at room temperature essentially as described (Marks et al., 1995) or with methanol at –20°C for 5 minutes followed by immunostaining. Cells were analysed on a Leica Microsystems (Bannockburn, IL) DM IRBE microscope using a Hamamatsu (Hamamatsu, Japan) Orca digital camera and Improvision OpenLab software (Lexington, MA). Most images shown are compressed from multiple deconvolved layers from a *z*-axis series of images taken at 0.2 μm increments. Quantitation of overlap for STxB and Golgi markers was done on non-deconvolved images using the Density Slicing and Quantitation modules of the OpenLab software.

Video confocal microscopy

HeLa-GRASP65-EGFP were grown on glass-bottomed microwell dishes (MatTek, Ashland, MA). For controls, GRASP65-EGFP was accumulated at ER exit sites by treating cells as described above for brefeldin-A washout at 16°C. For nocodazole treatment, HeLa-GRASP65-EGFP were incubated on ice for 15 minutes followed by incubation with 5 μg ml^{-1} nocodazole at 37°C for 2 hours and during the analysis. For dynamitin overproduction and tGolgin-1 depletion, cells were transduced with plasmid or siRNA as described above and observed 2 days after transfection. Time-lapse *z*-axis series images (0.5 μm steps) were analysed at intervals of 20 seconds (control) or 60 seconds (all others) in a 37°C heating chamber on a Ultraview LCI Nipkow disc confocal microscope (Perkin-Elmer, Norwalk, CT) attached to a Nikon TE300 inverted microscope (Nikon, Melville, NY) fitted with a 60× oil-immersion objective, as described (Whiteman et al., 2003) or on a Leica DM IRBE microscope using a Hamamatsu Orca digital camera. Captured images were analysed using Improvision OpenLab software (Lexington, MA). The distance that each mobile Golgi element moved per minute in each condition was assessed by comparing sequential images using OpenLab software. Statistical analyses used Stat2000.xls (S. Yamazaki) and Microsoft Excel software.

Electron microscopy

HeLa cells transduced twice with siRNA-1 or control siRNA were split into 10 cm dishes and fixed 2 days after the second transfection using 1.5% glutaraldehyde, 3% formaldehyde as described (McCaffery and Farquhar, 1995; Yoshino et al., 2003). Parallel analyses by IFM indicated that 85% of the cells transduced with siRNA-1 had undetectable levels of tGolgin-1 production. Cells were osmicated, embedded in epon, sectioned and analysed on a Philips 420 transmission electron microscope as described (McCaffery and Farquhar, 1995; Yoshino et al., 2003). Morphometry was performed on random images of phenotypic cells from the siRNA-1 sample and of random cells in the control sample using analySIS v3.2 software (Soft Imaging System, Lakewood, CO).

Immunoblotting

Immunoblotting of Triton-X-100 cell lysates fractionated by SDS-PAGE on 7.5% acrylamide gels was performed essentially as described (Berson et al., 2003) using mouse anti-p230 antibodies, enhanced chemiluminescence detection system (Amersham Pharmacia Biotech, Piscataway, NJ) and analysis on a Molecular Dynamics Storm 860 PhosphorImager (Amersham Pharmacia Biotech). As loading controls, blots were probed with anti-tubulin antibodies.

Results

Depletion of endogenous tGolgin-1 using siRNA

To probe tGolgin-1 function, we analysed the Golgi and TGN in HeLa cells after depleting tGolgin-1 using inhibitory RNA. siRNAs were designed corresponding to various regions within the coding sequence and 3′-untranslated region of human tGolgin-1-encoding mRNA (Fig. 1A). tGolgin-1 levels were undetectable by IFM in up to 60% of HeLa cells transduced once with siRNA-1 (Fig. 1B). After transfecting twice with siRNA-1 on consecutive days, tGolgin-1 was undetectable by IFM in up to 80-85% of HeLa cells and total tGolgin-1 protein levels were reduced by up to 80%, relative to control cells, as determined by western blotting (Fig. 1E). Transduction with control siRNA to an unrelated protein had no effect on tGolgin-1 production either by IFM or western blotting (data not shown; see below), and transduction with siRNA-1 had no effect on the production of several control proteins, including the GRIP protein golgin-97 (see below). We therefore concluded that tGolgin-1 production was effectively and specifically downregulated by siRNA-1 transduction. Similar IFM results were obtained in a smaller proportion of cells using two additional siRNAs (siRNA-2 and siRNA-3; Fig. 2A-F), whereas other tGolgin-1-directed siRNAs were either less potent (siRNA-4) or completely ineffectual (siRNA-5; data not shown).

tGolgin-1 depletion results in dispersal of the Golgi to peripheral mini stacks

In many siRNA-1-transduced cells that had undetectable levels of tGolgin-1 production, the distribution of the TGN integral-membrane protein TGN46 was significantly altered relative to controls by IFM (Fig. 1B,C, Fig. 2A,B, Fig. 3B,C). Its normal tight, centralized, ribbon-like pattern, characteristic of the TGN and Golgi in HeLa cells, was replaced by a vesicular pattern throughout the cell body. By quantitation of images from cells transduced once with siRNA-1, TGN46 was dispersed in at least 50-65% of cells that lacked detectable tGolgin-1 production, but not in any of the cells in the same culture in which tGolgin-1 production persisted or in cells transduced with control siRNAs (Fig. 1D). Dispersed TGN46 labelling was also observed upon depletion of tGolgin-1 using siRNA-2 and siRNA-3 directed to tGolgin-1 (Fig. 2A,B) but not in cells treated with siRNA-4, which reduced tGolgin-1 production only modestly, or with siRNA-5, which had no effect on tGolgin-1 production (data not shown). TGN46 dispersal, albeit more modest, was also observed upon depletion of tGolgin-1 in two melanoma cell lines (data not shown), indicating that this effect was not limited to HeLa cells. Finally, TGN46 dispersal was not observed in cells depleted of endogenous tGolgin-1 by siRNA-1 transduction but in which exogenous (siRNA-1-resistant) mouse tGolgin-1 was produced to reconstitute tGolgin-1 levels (Fig. 2G-I). By contrast, dispersal was clearly apparent in parallel cultures transduced with siRNA-1 and a control plasmid producing Rab27a (Fig. 2J-L). Taken together, these

data indicate that tGolgin-1 depletion results in disruption of TGN46-containing membranes into smaller vesicular structures in a large proportion of cells.

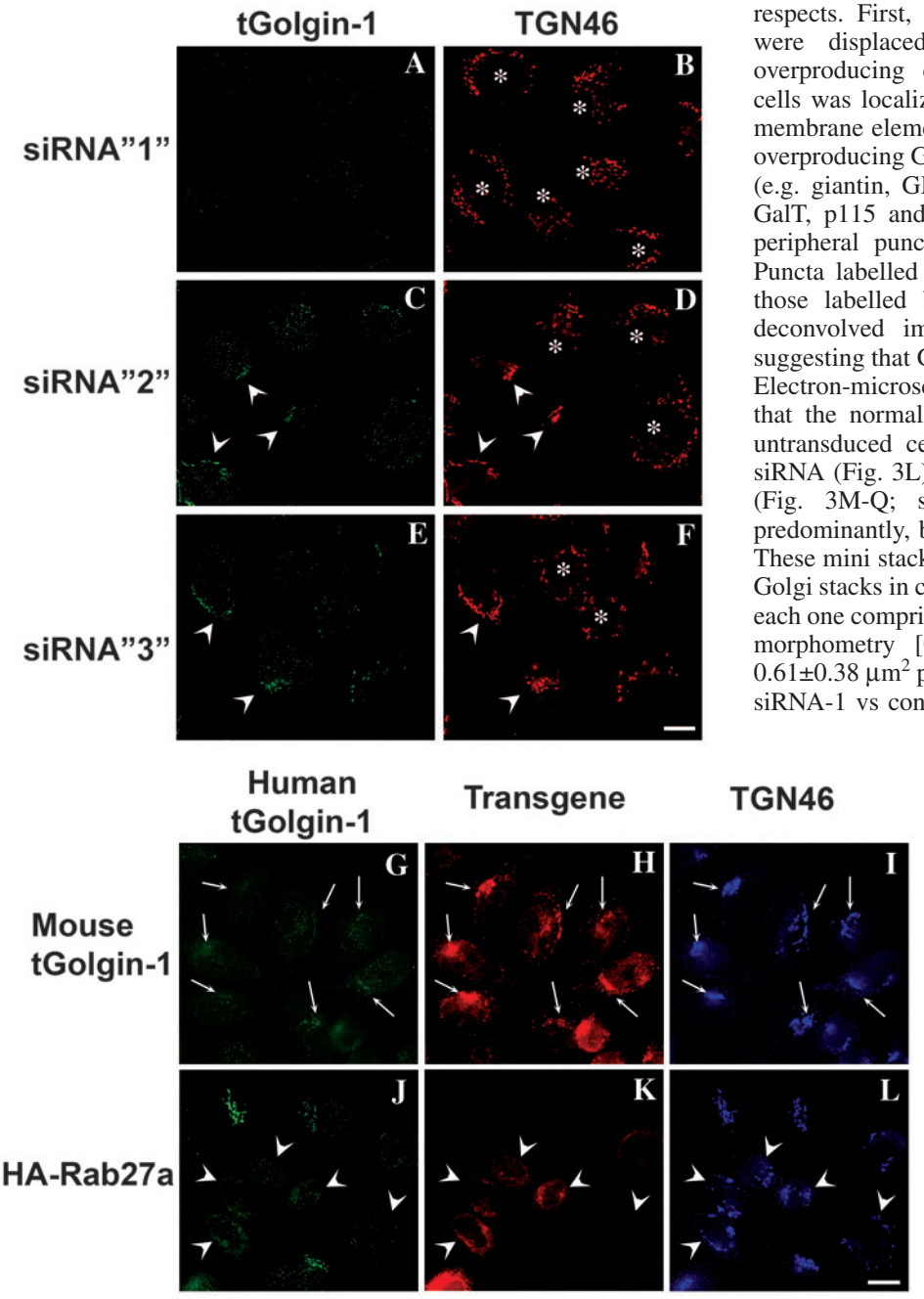

Fig. 2. Dispersed TGN46 is a function of tGolgin-1 depletion. (A-F) HeLa cells transduced once with siRNA-1 (A,B), siRNA-2 (C,D) or siRNA-3 (E,F) were fixed 2 days later and analysed by IFM for endogenous tGolgin-1 (A,C,E) and TGN46 (B,D,F). Stars denote cells without tGolgin-1 labelling and arrowheads denote cells with significant residual levels of tGolgin-1. (G,H) HeLa cells were co-transduced with siRNA-1 and plasmids encoding either siRNA-1-resistant mouse tGolgin-1 (G-I) or irrelevant HA-epitope tagged Rab27a (J-L), then fixed 2 days later and analysed by IFM using antibodies specific for human tGolgin-1 (G,J), for both human and mouse tGolgin-1 (H,K), and for TGN46 (I,L), and appropriate fluorochrome-conjugated secondary antibodies. Arrows (G-I) denote cells with negligible labelling for endogenous human tGolgin-1 but that are reconstituted with mouse tGolgin-1; notice the ribbon-like labelling of TGN46. Arrowheads (J-L) denote cells with negligible labelling for endogenous human tGolgin-1; notice the dispersed TGN46 labelling in most of these cells.

TGN46 dispersal has also been observed in cells overproducing dominant-negative GRIP domains from tGolgin-1 and golgin-97 (Yoshino et al., 2003). However, the phenotype of tGolgin-1-depleted cells differed in several respects. First, whereas both tGolgin-1 and golgin-97 were displaced to the cytosol in GRIP-domain-overproducing cells, golgin-97 in tGolgin-1-depleted cells was localized to the peripheral TGN46-containing membrane elements (Fig. 3C,D). Second, unlike in cells overproducing GRIP domains, markers of the Golgi stack (e.g. giantin, GM130 and GS28; and also, not shown, GalT, p115 and GRASP65) were also redistributed to peripheral puncta, as observed by IFM (Fig. 3E-K). Puncta labelled for Golgi markers partially overlapped those labelled by TGN46 in a polarized manner in deconvolved images of *z*-axis sections (Fig. 3I-K), suggesting that Golgi cis→trans polarity was maintained. Electron-microscopic analysis of these cells indicated that the normally centralized Golgi complex found in untransduced cells or cells transduced with a control siRNA (Fig. 3L) was replaced by multiple 'mini stacks' (Fig. 3M-Q; see also Fig. 8) that were present predominantly, but not exclusively, at the cell periphery. These mini stacks were morphologically similar to intact Golgi stacks in control cells but were more numerous and each one comprised a smaller total area, as determined by morphometry [0.20±0.10 μm^2 per stack (n=31) vs 0.61±0.38 μm^2 per stack (n=15) for cells transduced with siRNA-1 vs control siRNA, respectively]. In contrast to Golgi and TGN residents, the distribution of resident proteins of other compartments, including ER, early endosomes, recycling endosomes, late endosomes and lysosomes, was not affected by tGolgin-1 depletion (see Fig. S1 in supplementary material; however, see Fig. 8 regarding the morphology of late endosomes and lysosomes), and the uptake and intracellular accumulation of transferrin was not perceptibly altered (data not shown). These data indicate that the Golgi/TGN was specifically decentralized in cells depleted of tGolgin-1.

tGolgin-1 depletion mimics dynein-dynactin disruption

Polarized Golgi mini stacks are also observed in cells in which microtubule dynamics are disrupted by depolymerization with nocodazole (Cole et al., 1996a; Storrie et al., 1998) or by overproduction of the dynamitin p50 subunit of the dynein-dynactin motor complex (Burkhardt et al., 1997). In these cells, pre-Golgi elements that form upon fusion of membranes from ER-derived vesicles fail to migrate along microtubules

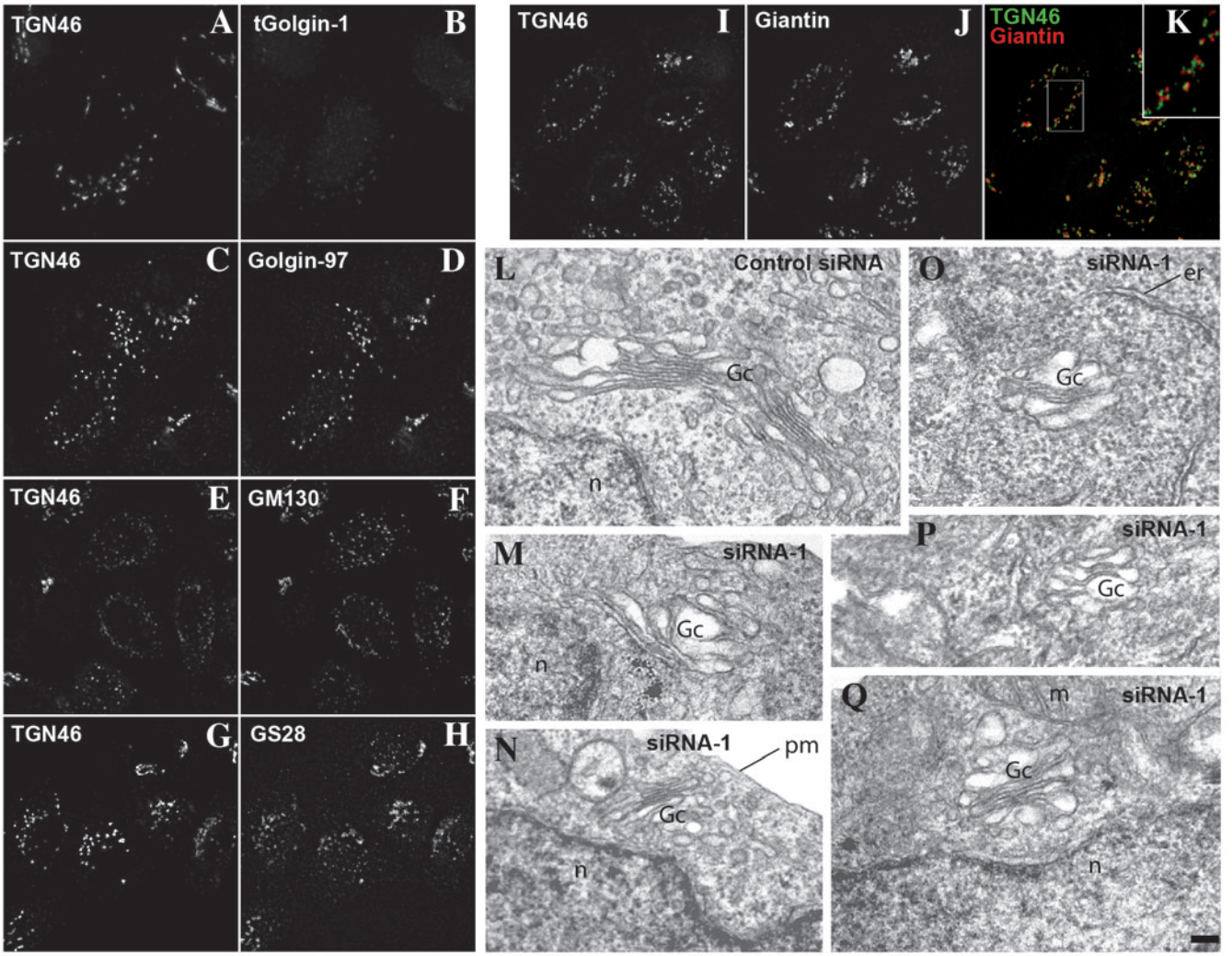

Fig. 3. Dispersal of TGN and Golgi elements in cells depleted of tGolgin-1. HeLa cells transduced twice with siRNA-1 were fixed 1 day later. They were then either analysed by IFM using primary antibodies to TGN46 and to the indicated proteins, followed by the appropriate fluorochrome-conjugated secondary antibodies (A-K), or embedded in epon and analysed by electron microscopy. (C-K) tGolgin-1-depleted cells were identified based on the dispersed pattern of TGN46 staining. (K) A colorized overlay of the images shown in I,J to emphasize the polarity of the Golgi and TGN elements; the boxed region is magnified 2.5 times in the top right corner. (L-Q) Characteristic electron microcopy fields containing Golgi membranes in cells transduced with control siRNA (L) or siRNA-1 (M-Q). Notice the reduced size of the stacks in cells transduced with siRNA-1. Bar in Q (applies to L-Q), 0.2 μm.

towards the MTOC, resulting in the reformation and accumulation of functional Golgi-like structures near ER exit sites (Hammond and Glick, 2000). Indeed, parallel IFM analyses of cells depleted of tGolgin-1 (Fig. 3A-K), cells treated with nocodazole or cells overproducing dynamitin (Fig. 4S-X and data not shown) showed similar profiles. The following experiments were done to test whether the Golgi fragments resulting from tGolgin-1 depletion similarly resulted from a failure to transport pre-Golgi intermediates along microtubules towards the MTOC.

First, parallel staining for Golgi and/or TGN markers and microtubules showed that, as in dynamitin-overproducing cells, microtubules were intact and the Golgi-like elements in tGolgin-1-depleted cells appeared to be aligned along them (Fig. 4A-F). Second, using γ-tubulin as a marker for the MTOC, we asked whether Golgi elements remained clustered near the MTOC as they do in untreated cells (Fig. 4G-I). Although the Golgi was largely dispersed to peripheral stacks in cells treated with nocodazole, large clusters of Golgi remnants harbouring GalT-EGFP were colocalized with γ-tubulin (Fig. 4J-L), suggesting that a significant population of Golgi fragments remained associated with nocodazole-insensitive ‘stubs’ of microtubules at the MTOC. By contrast, in cells that either overproduced dynamitin-p50 (Fig. 4M-O) or were depleted of tGolgin-1 by siRNA-1 (Fig. 4P-R), no such remnants accumulated near the MTOC. This difference between nocodazole-treated and either dynamitin-overproducing or tGolgin-1-depleted cells was particularly evident using giantin as a marker (compare Fig. 3J with Fig. 4S-X). The data support the notion that nocodazole treatment and dynamitin overproduction distinguish two phases in Golgi accumulation at the MTOC, a transport phase (dependent on dynein-dynactin) and a subsequent tethering phase. Importantly, tGolgin-1 depletion mimics dynamitin

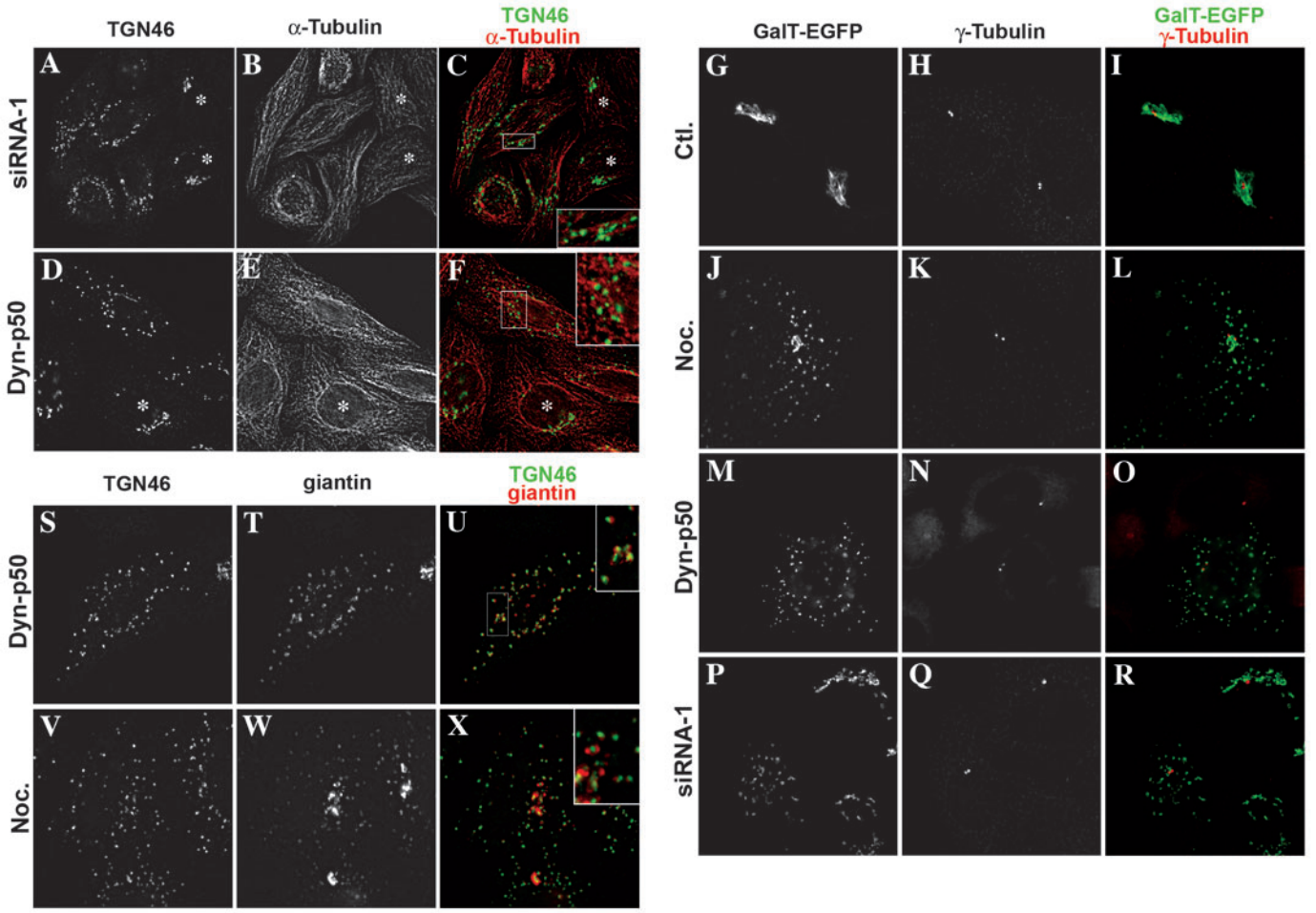

Fig. 4. Association of Golgi elements with microtubules in cells depleted of tGolgin-1. (A-F) HeLa cells transduced twice with siRNA-1 (A-C) or with dynamitin-p50 (D-F) were fixed 1-2 days later and analysed by deconvolution IFM using primary antibodies to TGN46 and α-tubulin. (C,F) Overlays of the two labels. The boxed regions are magnified 2.5 times in the bottom or top right corner to emphasize the alignment of Golgi elements along microtubules. (G-R) HeLa cells were transfected with GalT-EGFP alone and left untreated (Ctl.; G-I) or treated with nocodazole (Noc.; J-L), or cotransfected with GalT-EGFP and dynamitin-p50 (Dyn-p50; M-O) or with GalT-EGFP and siRNA-1 (P-R). Cells were fixed, labelled with anti-γ-tubulin and RRX-conjugated secondary antibodies, and analysed by deconvolution fluorescence microscopy. Colorized overlays of the two labels are shown on the right. (S-X) Untransduced cells treated for 2 hours with nocodazole (Noc.; V-X) or cells transfected with dynamitin-p50 (S-U) were fixed and analysed by deconvolution IFM using primary antibodies to TGN46 and giantin. (U,X) Overlays of the two labels; the boxed regions are magnified 2.5 times in the top right corners.

overproduction, suggesting that tGolgin-1 production might be required for the transport phase of Golgi elements toward the minus end of microtubules.

To determine the proximity of Golgi-like elements to ER exit sites in tGolgin-1-depleted cells, the redistributed Golgi and TGN markers were compared with the distribution of Sec13-EGFP (an EGFP-conjugated subunit of the COPII coat complex that marks these sites) (Hammond and Glick, 2000). In cells co-transfected with low levels of Sec13-EGFP and siRNA-1 (Fig. 5A-C) or treated with nocodazole (Hammond and Glick, 2000) (Fig. 5D-F), TGN46- and giantin-labelled vesicles cluster around elements labelled by Sec13-EGFP, indicating that Golgi/TGN elements indeed accumulate near ER exit sites in these cells.

To determine whether secretory transport through the Golgi complex is affected by tGolgin-1 depletion, we assessed the migration of the ts045 temperature-sensitive variant of VSV-G (Bergmann et al., 1981) conjugated to EGFP (Presley et al., 1997) from the ER to the cell surface. In cells co-transfected with VSV-G/EGFP and either siRNA-1 (Fig. 5G-L) or high levels of dynamitin (see Fig. S2 in supplementary material), VSV-G/EGFP accumulated normally in the ER at 39°C; after a shift to 32°C, VSV-G/EGFP was accumulated primarily in the peripheral Golgi elements after 30 minutes, and then at the plasma membrane by 60 minutes. These kinetics were virtually identical to those of VSV-G/EGFP in untreated cells (see Fig. S2 in supplementary material), consistent with previous reports in nocodazole-treated cells (Rogalski and Singer, 1984). Thus, the disruption of Golgi architecture induced by tGolgin-1 depletion did not affect Golgi function in secretory transport.

Finally, we analysed the effects of tGolgin-1 depletion on Golgi element motility using video microscopy. An EGFP-tagged form of the Golgi matrix protein GRASP65 (Lane et al., 2002) was stably produced in HeLa cells and individual clones were chosen that had predominant Golgi localization by fluorescence microscopy. The cells were then analysed by

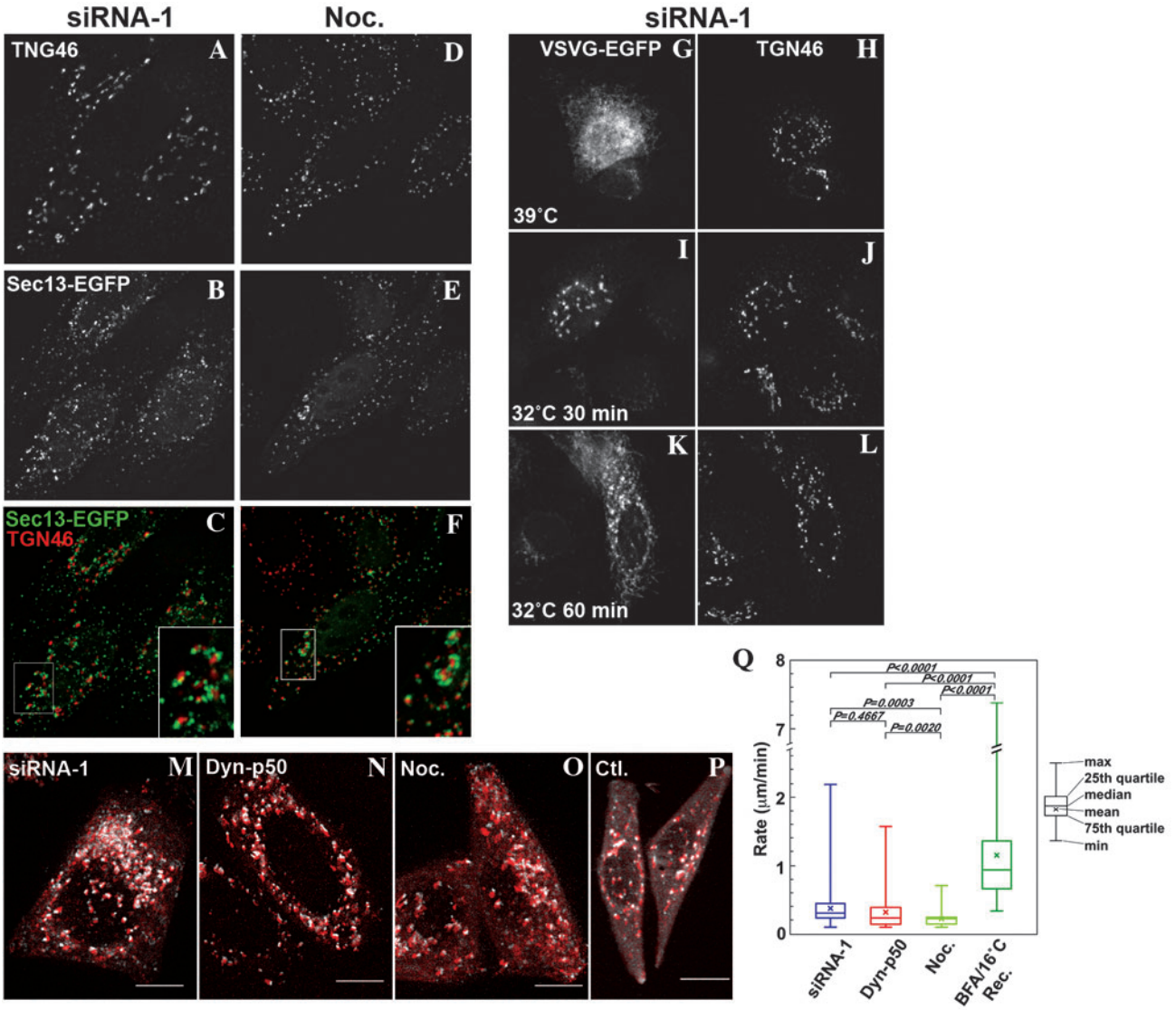

Fig. 5. tGolgin-1 depletion mimics disruption of dynein-dynactin or microtubules in terms of Golgi element position, function and movement. (A-F) HeLa cells transduced with both siRNA-1 and plasmid encoding Sec13-EGFP (A-C) or Sec13-EGFP alone (D-F) were fixed 2 days later without (A-C) or with (D-F) treatment with nocodazole (Noc.) for 2 hours, and analysed by fluorescence microscopy after labelling with anti-TGN46 and RRX-conjugated secondary antibody. Individual labels are shown in A,B,D,E, and the overlay is shown in C,F; the boxed region in C is magnified 2.5 times in the bottom right corner. tGolgin-1-depleted cells were identified based on the labelling pattern for TGN46. Notice the accumulation of TGN46 labelling near sites labelled by Sec13-EGFP. (G-L) HeLa cells transduced with both siRNA-1 and plasmid encoding VSV-G/EGFP were incubated overnight at 39°C and then fixed either immediately (G,H) or after a 30 minute (I,J) or 60 minute (K,L) incubation at 32°C. Cells were analysed by fluorescence microscopy after labelling with anti-TGN46 and RRX-conjugated secondary antibody. tGolgin-1-depleted cells were identified based on the labelling pattern for TGN46. Notice the appearance of cell-surface labelling (particularly in surface spikes) for VSV-G/EGFP by 60 minutes. (M-P) HeLa cells stably expressing GRASP65-EGFP were transduced transiently with siRNA-1 (M) or dynamitin-p50 (n), treated with nocodazole for 2 hours (O), or exposed to brefeldin A for 1 hour, washed, recovered at 16°C for 3 hours and then released at 37°C (P). Cells were analysed by video microscopy and representative images were collected every 60 seconds (M-O) or 20 (P) seconds for 5 minutes. Images from all time points were overlaid, with the initial image labelled in white and all subsequent images labelled in red to indicate movement from the initial position. Notice that very few labelled elements in m-o showed significant movement over the 5 minute time course. (Q) Quantitation of Golgi element movement. 50-150 spots from at least five cells in each experimental sample represented in m-p were analysed for distance moved over the 5 minute time course. The mean, median, maximum (max) and minimum (min) values, and 25th and 75th quartile values for distance moved in each experimental set are shown. Pairs of value sets were analysed by Student's *t* test, and *P* values for each paired analysis are indicated.

video microscopy after treatment with nocodazole or after transduction with siRNA-1 or dynamitin expression vector, and summary images of representative videos were prepared in which EGFP signal in the initial frame is coloured white and subsequent frames are coloured red (Fig. 5M-O). The results demonstrate that GRASP65-containing elements in all three sets of cells were relatively immobile. As a control, we performed similar analyses of cells in the process of

Table 2. Proportions of static and mobile GRASP65-EGFP elements in tGolgin-1-depleted, dynein/dynactin-disrupted, microtubule-disrupted and control cells

	RNA interference*	Dynamitin*	Nocodazole*	Brefeldin-A recovery‡
Static	6.91%	26.15%	42.13%	27.80%
Mobile	93.09%	73.85%	57.87%	72.20%
Sample size(*n*)	753	348	235	313

*During 1 minute
‡During 20 seconds

recovering at 16°C from brefeldin-A treatment. Although some of the larger elements in these cells were also relatively immobile during the course of the experiment, the majority of them and most of the smaller elements were highly motile (Fig. 5P). Quantitation of the movement of random individual elements from all experimental samples (Table 2, Fig. 5Q) confirms that both the proportion of motile elements and the median rate of movement were similar in siRNA-1-treated and dynamitin-overproducing cells, much lower than in control cells and slightly higher than in nocodazole-treated cells. Taken together, these data show that the Golgi elements formed in the presence of siRNA-1 are relatively immobile and similar to those that form in the absence of dynein-dynactin motor function. The results are consistent with a requirement for tGolgin-1 in minus-end-directed motility of Golgi elements along microtubules rather than in the retention or tethering of motile Golgi elements at the MTOC.

tGolgin-1 does not directly function in Golgi motility

For Golgi elements to migrate toward the MTOC, they must recruit and activate dynein-dynactin motor complexes (Burkhardt et al., 1997; Corthesy-Theulaz et al., 1992; Harada et al., 1998). Thus, a simple potential explanation for the data presented thus far is that tGolgin-1 is part of a tether for dynein-dynactin complexes on pre-Golgi membranes. However, this belies the steady-state localization of tGolgin-1 and other GRIP proteins at the TGN (Brown et al., 2001; Gleeson et al., 1996; Luke et al., 2003; Panic et al., 2003b; Setty et al., 2003). Furthermore, we were unable to detect interactions between tGolgin-1 and any dynein-dynactin subunit using a range of biochemical approaches with cell lysates or

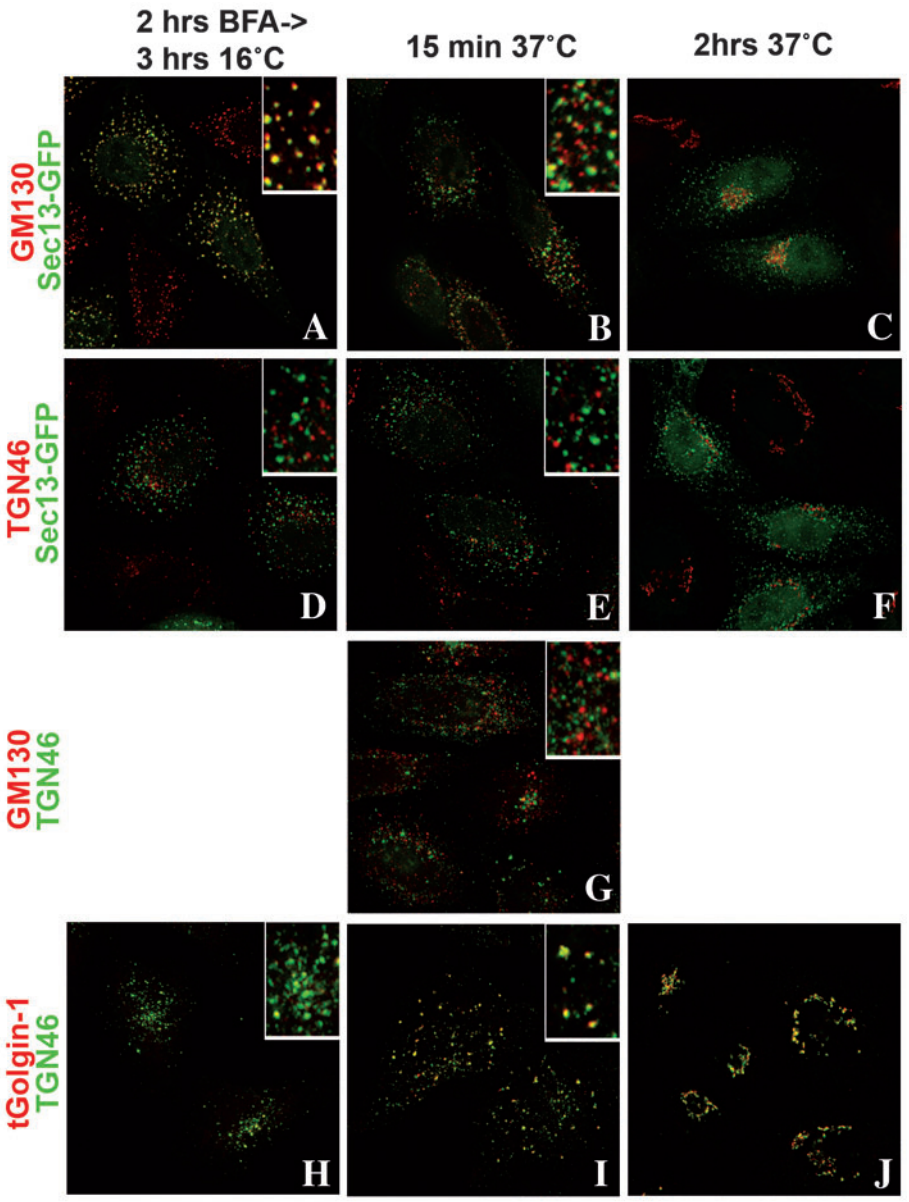

Fig. 6. The requirement for tGolgin-1 in microtubule minus-end-directed movement of pre-Golgi intermediates is indirect. HeLa cells transduced with Sec13-EGFP (A-F) or untransduced HeLa cells (G-J) were treated for 1 hour with 1 μg ml^{-1} brefeldin A (BFA) and then washed and incubated at 16°C for an additional 3 hours in the absence of BFA. Cells were then fixed immediately or after an additional incubation at 37°C for 15 minutes to 2 hours, and analysed by IFM after labelling with antibodies to the indicated proteins and appropriate fluorochrome-conjugated secondary antibodies. Only the overlaid images from both labels are shown. (A-F) Comparison of the ER exit site marker Sec13-EGFP and either Golgi (GM130; A-C) or TGN (TGN46; D-F) elements at all three time points. (G) Comparison of Golgi (GM130) and TGN (TGN46) elements at the 15 minute time point. (H-J) Comparison of tGolgin-1 and TGN (TGN46) elements at all time points. Boxed regions in the top right corner of A,B,D,E,G-I represent 2.5 times magnified images from the corresponding panels to emphasize the degree of colocalization. Notice that, whereas GM130 initially localizes to Sec13/EGFP-containing structures before migrating towards the MTOC, TGN46 and tGolgin-1 initially localize to separate structures that remain separate during transport.

recombinant proteins (data not shown). To rule out the possibility that transient and/or indirect interactions that might have eluded our detection occur in vivo, we tested whether tGolgin-1 was present on newly forming pre-Golgi intermediates that form near ER exit sites. Pre-Golgi intermediates were accumulated in HeLa cells by treatment with brefeldin A at 37°C followed by incubation at 16°C in the absence of brefeldin A. After 3 hours at 16°C following brefeldin-A washout, peripheral punctate Golgi elements marked by GM130 were localized to ER exit sites marked by Sec13-EGFP (Fig. 6A) as described (Hammond and Glick, 2000). By 15 minutes at 37°C, these elements had largely segregated from ER exit sites and no longer colocalized with Sec13-EGFP (Fig. 6B); by 2 hours, they had converged to a ribbon-like structure near the MTOC (Fig. 6C). TGN elements, marked by TGN46, were also distributed as peripheral puncta after 3 hours at 16°C but the puncta did not localize to ER exit sites (Fig. 6D); these puncta might correspond to part of an endosomal network (Reaves and Banting, 1992; Wagner et al., 1994), although they only minimally overlapped with transferrin receptors (data not shown). The TGN46-containing puncta also appeared to coalesce, intensify and migrate toward the MTOC by 15 minutes at 37°C (Fig. 6E) but remained distinct from the Golgi puncta (Fig. 6G) until 2 hours at 37°C, when both Golgi and TGN elements coalesced near the MTOC (Fig. 6C,F) as in untreated cells. Importantly, tGolgin-1 [which was not detected on membranes after 3 hours at 16°C following brefeldin-A treatment (Fig. 6H)] was recruited to TGN46-containing puncta, not the GM130-containing Golgi puncta, after 15 minutes at 37°C (Fig. 6I). As expected, by 2 hours of recovery, tGolgin-1 and TGN46 were extensively colocalized in ribbon-like structures near the MTOC (Fig. 6J). These data indicate that GM130-containing pre-Golgi elements migrate towards the MTOC independently of tGolgin-1-containing TGN elements. Because the motile pre-Golgi elements lack tGolgin-1, the requirement for tGolgin-1 in pre-Golgi movement must not reflect any direct role as part of a linker complex between Golgi elements and microtubule motors. Rather, the requirement must reflect an indirect effect of tGolgin-1 production, probably on the recruitment or activation of dynein/dynactin complexes.

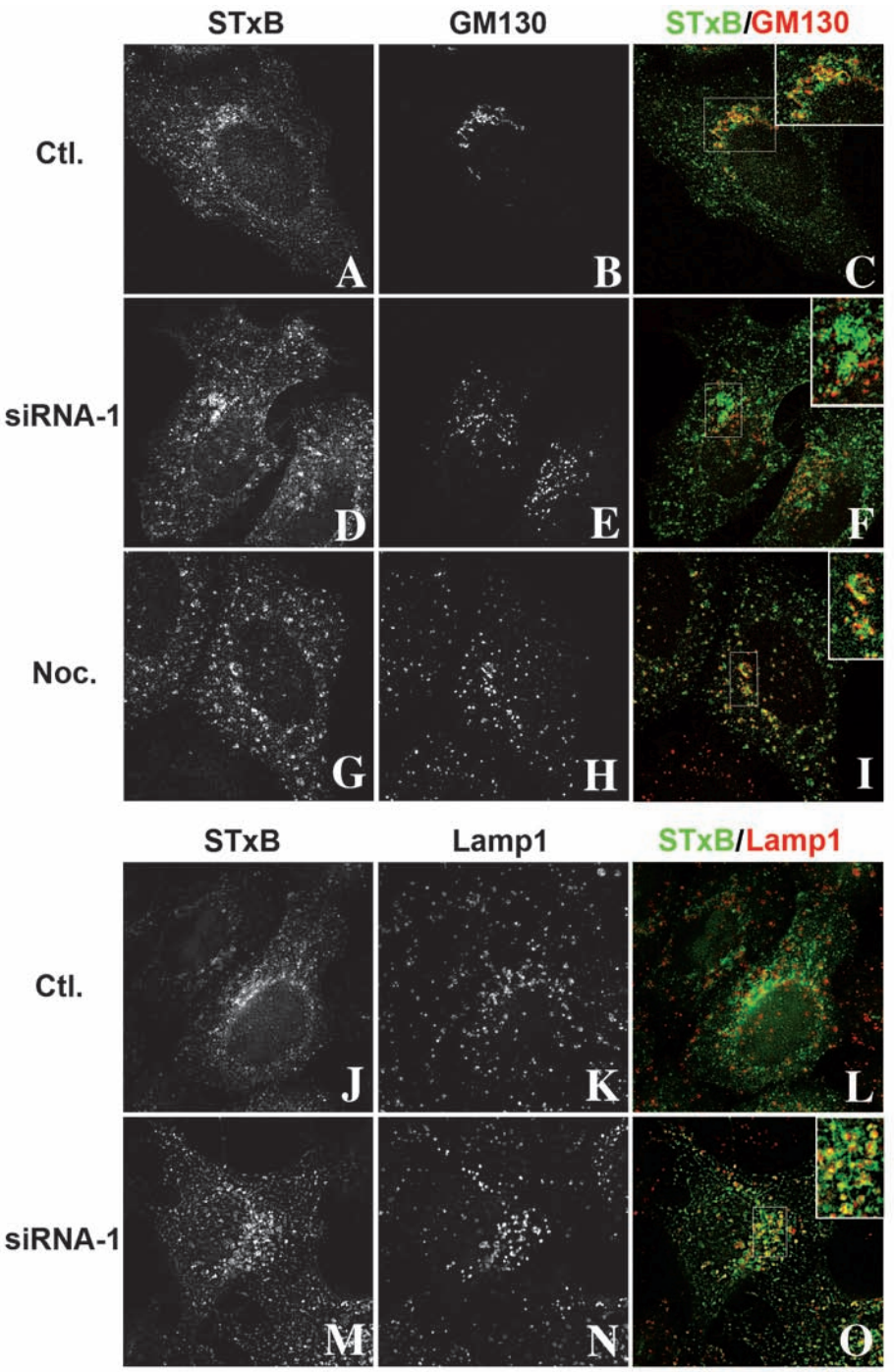

Fig. 7. Endosome-to-Golgi transport of STxB is inhibited by tGolgin-1 depletion. HeLa cells that were untreated (Ctl.), transduced with siRNA-1 or treated for 2 hours with nocodazole (Noc.) were incubated with Alexa-488-conjugated STxB on ice for 45 minutes, washed and then warmed to 37°C for 60 minutes. Cells were then fixed, labelled with antibodies to GM130 and RRX-conjugated anti-mouse immunoglobulin (A-I) or to TGN46 and Lamp1 followed by AMCA- and RRX-conjugated secondary antibodies (J-O), and analysed by fluorescence microscopy. siRNA-1-transduced cells were identified based on the dispersed staining pattern for TGN46. Panels show single staining for STxB (A,D,G,J,M), GM130 (B,E,H) or Lamp1 (K,N), or overlays of the two labels, as indicated (C,F,I,L,O). Boxed images were magnified two-fold in the top right corner in C,F,I,O to emphasize the degree of colocalization.

Table 3. Proportions of area colocalized with STxB in GM130-positive structures*

Control (untransfected)	33.66±15.98% (*n*=14)
Nocodazole treated	35.25±14.26% (*n*=19)
siRNA-1 transduced	17.10±13.82% (*n*=17)

*Values represent the proportions of GM130-containing pixels within the number (*n*) of cells shown that also contain STxB.

tGolgin-1 modulates retrograde transport of Shiga toxin from endosomes

How might tGolgin-1 indirectly regulate Golgi motility? Given the role of other GRIP proteins in recycling of TGN-resident proteins from endosomes and/or maintaining TGN structure (Li and Warner, 1996; Lu et al., 2004; Siniossoglou et al., 2000; Tsukada et al., 1999; Yoshino et al., 2003), we postulated that tGolgin-1 itself might function in a pathway required for recycling a factor(s) required for dynein-dynactin recruitment or activation. To assay endosome-to-Golgi transport, we followed internalized, Alexa-488-conjugated STxB. STxB binds to the glycosphingolipid Gb3 at the plasma membrane and, following internalization with Gb3, undergoes sequential rounds of retrograde transport, eventually to the ER (Johannes and Goud, 1998). Importantly, retrograde delivery of STxB from endosomes to the TGN occurs via early and recycling endosomes (Mallard et al., 1998), similar to TGN38/46 (Ghosh et al., 1998).

HeLa cells were incubated with Alexa-488-conjugated STxB at 0°C for 45 minutes, washed and then warmed to 37°C for 60 minutes to permit internalization of the bound STxB. In control cells, a large proportion of the STxB at this time point colocalized with GM130 at the Golgi (Fig. 7A-C). By contrast, a much smaller proportion of STxB colocalized with GM130 in dispersed Golgi structures in cells depleted of tGolgin-1 (Fig. 7D-F; notice that at no time was significant colocalization of STxB with TGN46 observed in data not shown). Quantitation of the proportion of the total GM130-containing cell area that also contained STxB showed at least a halving of the ability of STxB to reach the Golgi in tGolgin-1-depleted cells (Table 3); this is probably an underestimate of the defect based on the method of quantitation used. The defect in transport was not an indirect effect of Golgi dispersal, because STxB localized efficiently to GM130-containing puncta in control cells treated with nocodazole (Fig. 7G-I, Table 3). The decrease in STxB transport to Golgi elements was compensated by an increased colocalization with early endosomal markers transferrin receptor and EEA1 (see Fig. S3 in supplementary material) and, importantly, a dramatic increase in colocalization with perinuclear late endosomes marked by Lamp1 (Fig. 7J-O). These data indicate that, in the absence of tGolgin-1, STxB is inefficiently distributed to the Golgi from early endosomes and is significantly mis-sorted to late endosomes.

STxB trafficking probably reflects the intracellular itinerary of its glycosphingolipid ligand (Sandvig and van Deurs, 2002), and indeed we observed similar lysosomal mis-sorting of an internalized synthetic glycosphingolipid analogue, *N*-[5-(5,7-dimethyl BODIPY)-1pentanoyl]-lactosylceramide (data not shown), although the effect was difficult to quantify. If tGolgin-1 was required for post-endocytic sorting of glycolipids then cells lacking tGolgin-1 would be predicted to accumulate unusual late endosomal membrane structures owing to the increased content of glycolipids and their associated cholesterol, as is observed in cells from patients with lysosomal lipid-storage diseases (Marks and Pagano, 2002). Consistent

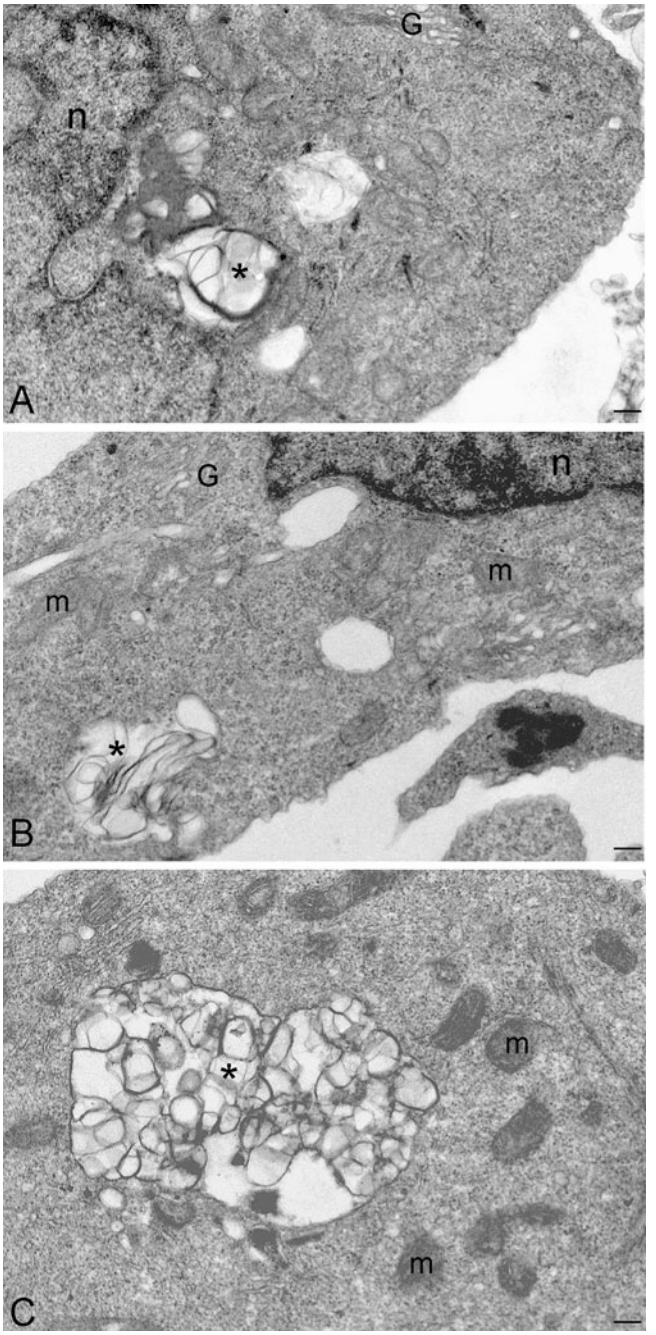

Fig. 8. Accumulation of aberrant multivesicular structures in tGolgin-1-depleted cells. HeLa cells transduced twice with siRNA-1 were fixed 1 day later and processed for conventional electron microscopic analysis. Typical fields are shown from these cells containing aberrant vacuolar structures (*), which appear to be derived from multilaminar (A,B) or multivesicular (C) endosomes. Notice the peripheral Golgi mini stack (G) in A. m, mitochondria; n, nucleus. Bar, 1 μm.

with this prediction, ultrastructural analysis of tGolgin-1-depleted cells revealed an abundance of unusual large vacuolar structures with clumps of internal membranes in 'whorls' (Fig. 8A,B) or vesicle-like profiles (Fig. 8C), much like those found in lipid-storage-disease patients (Marks and Pagano, 2002). Quantification showed that whorls were found in seven out of 123 random images from tGolgin-1-depleted cells, but none out of 51 random images of cells treated with a control siRNA. Although the morphology of these compartments was altered, the distribution of most lysosomal proteins to them was not adversely affected (see Fig. S1 in supplementary material). These data support the interpretation that internalized glycosphingolipids are significantly mis-sorted to late endosomes/lysosomes in cells depleted of tGolgin-1, and implicate tGolgin-1 in regulating the retrograde transport of glycolipids.

Discussion

The positioning of the Golgi complex near the MTOC requires first the recruitment and activation of the dynein/dynactin complex to allow migration of pre-Golgi membranes towards the MTOC along microtubules, and then tethering of Golgi membranes to the MTOC upon their arrival and maturation. Our data provide novel evidence that tGolgin-1 function is required for the first step to ensure correct positioning of Golgi membranes at the MTOC. However, its absence from migrating pre-Golgi membranes indicates that tGolgin-1 is not itself part of the motor recruitment complex but rather functions in a regulatory role in the localization, organization or activation of the complex. Because we also show that tGolgin-1 is required for the distribution of internalized STxB from endosomes to the Golgi and that interference with other factors required for endosome-to-Golgi recycling also results in Golgi dispersal, we suggest that endosome-to-Golgi recycling regulates the localization and/or activity of factors required for Golgi motility towards the MTOC.

'Dispersal' of Golgi-resident proteins, as observed by fluorescence microscopy, can result from any number of insults to the Golgi complex, including disruption of vesicular traffic, cisternal stacking, organelle motility or tethering to the MTOC (Warren and Shorter, 2002). Our data indicate that tGolgin-1 production is required specifically for the movement of Golgi or pre-Golgi elements toward the MTOC. First, the microtubule network in cells lacking tGolgin-1 was intact and Golgi elements appeared to be associated with them, ruling out any gross effects on microtubule organization or Golgi-associated microtubule-binding proteins, as might be predicted from the observed in vitro interactions of tGolgin-1 with the actin/microtubule-binding protein ACF7/MACF1 (Kakinuma et al., 2004). Second, unlike depletion of the Golgi-vesicle tethering factor golgin-84 (Diao et al., 2003; Malsam et al., 2005), depletion of tGolgin-1 did not affect anterograde transport of VSV-G/EGFP. Third, the Golgi dispersal observed upon tGolgin-1 depletion mimics that observed upon interfering with the dynein-dynactin complex or microtubules (Burkhardt et al., 1997; Cole et al., 1996a; Hammond and Glick, 2000) in that polarized Golgi mini stacks accumulate at ER exit sites, the Golgi stacks remain functional for anterograde transport and motility is inhibited. Moreover, unlike in cells treated acutely with nocodazole in which dynein-dynactin function is intact and microtubules only transiently disrupted, tGolgin-1-depleted cells showed no Golgi fragments tethered at microtubule 'stubs' at the MTOC. Fourth, rapid bidirectional movement of Golgi elements along microtubules, as observed for untethered melanosomes in cells lacking Rab27a (Wu et al., 2001), was not observed in tGolgin-1-depleted cells, indicating a defect in motility that precedes tethering. Although we did not detect a quantitative decrease in dynein or dynactin subunits in pelletable fractions of HeLa cell homogenates upon tGolgin-1 depletion, as might be predicted if dynein-dynactin recruitment was inhibited, the minimal steady-state accumulation of these subunits at the Golgi in untreated cells (data not shown) renders this result uninterpretable and indicates that dynein-dynactin complexes associate dynamically with MTOC-bound pre-Golgi membranes in a manner that is not reflected by steady-state accumulation. We infer from the distinct phenotypes of chronic dynein-dynactin disruption (by dynamitin-p50 overproduction or tGolgin-1 depletion) and acute microtubule disruption (by nocodazole treatment) that tGolgin-1 function is required for dynamic association of Golgi membranes with an active motor complex.

How is tGolgin-1 function in Golgi migration exerted? The absence of tGolgin-1 from actively migrating Golgi/pre-Golgi elements bound for the MTOC in control cells indicates that tGolgin-1 is not a component of a receptor or activator for dynein-dynactin complexes on the cytoplasmic face of these elements. The unlikely possibility that a small, undetectable fraction of tGolgin-1 on these elements directly binds to dynein or dynactin is difficult to reconcile with the TGN localization of tGolgin-1 at steady state (Gleeson et al., 1996) and with our inability to detect interactions between tGolgin-1 and dynein or dynactin subunits using a range of biochemical approaches (data not shown). An indirect requirement for tGolgin-1 in Golgi motility is further supported by the failure to observe Golgi dispersal upon microinjection of antibodies against tGolgin-1 into HeLa cells, which resulted in a transient loss of detectable production of the endogenous protein (data not shown). Moreover, the heterogeneity of the response (50-65% of tGolgin-1-depleted cells showed Golgi dispersal) is inconsistent with a direct role. The proportion of tGolgin-1-depleted cells with Golgi dispersal was not dependent on time after transfection and was unchanged by inhibition of cell-cycle progression or by recovery after brefeldin-A treatment (data not shown), ruling out a requirement for mitotic or drug-induced Golgi dispersal before the tGolgin-1 requirement. We therefore favour a model in which tGolgin-1 acts indirectly by regulating the transient localization or activation of a crucial dynein-dynactin recruitment or activation factor.

How might tGolgin-1 regulate such a factor? We have shown here that cells depleted of tGolgin-1 mis-sort the internalized glycolipid ligand STxB to late endosomes/lysosomes and accumulate aberrant endosomal structures. These results imply that Golgi redistribution in tGolgin-1-depleted cells might be a secondary consequence of disrupting membrane recycling. This is consistent with the function of another GRIP-domain protein golgin-97 (Lu et al., 2004) and with results of dominant-negative GRIP-domain overproduction, in which endosome-to-TGN recycling was inhibited (Yoshino et al., 2003). Indeed, although depletion of some retrograde transport factors has no effect on Golgi morphology (Saint-Pol et al.,

2004), several groups have recently reported Golgi dispersal of an undefined nature after siRNA-mediated depletion of other factors regulating endosome-to-TGN transport, including retromer components (Seaman, 2004) and golgin-97 (Lu et al., 2004). We suggest that retrograde transport is required to localize membrane-associated factors that function directly in dynein-dynactin recruitment to pre-Golgi elements. Such factors might be either integral membrane proteins or lipids, both of which have been shown to cycle from endosomes to the Golgi (Ghosh et al., 1998; Johannes and Goud, 1998; Mallet and Maxfield, 1999), including to the cis Golgi (Natarajan and Linstedt, 2004), and might tether known dynein-dynactin recruitment proteins such as Bicaudal-D (Matanis et al., 2002; Short et al., 2002), βIII spectrin (Holleran et al., 2001) and CLIPR-59 (Perez et al., 2002). An intriguing possibility is that the relevant targets of retrograde transport are glycolipids and/or cholesterol. A consequence of chronic mis-sorting to late endosomes would be eventual depletion from the Golgi of recycling glycosphingolipids and probably concomitant depletion of associated cholesterol (Brown, 1998; Marks and Pagano, 2002; van Meer, 2002). Although glycosphingolipid deficiency per se does not result in Golgi dispersal (Sprong et al., 2001), depletion or enhancement of Golgi cholesterol is known to affect Golgi distribution and intra-Golgi transport (Stüven et al., 2003), as well as the requirement for the kinesin family member KIFC3 in Golgi motility (Xu et al., 2002). Cell-to-cell variation in cholesterol or glycosphingolipid content might explain why only 50-65% of tGolgin-1-depleted cells show Golgi dispersal, and cholesterol depletion might explain the reduced steady-state localization of a glycosylphosphatidylinositol-linked protein to the plasma membrane in cells overproducing a tGolgin-1-derived peptide (Kakinuma et al., 2004).

The localization of internalized STxB to the Golgi was impaired but not ablated in tGolgin-1-depleted cells, indicating that tGolgin-1 production facilitates but is not required for retrograde transport. Indeed, tGolgin-1 might influence retrograde transport indirectly. The mis-sorting of STxB to late endosomes is distinct from the early-endosome accumulation observed upon direct inhibition of the endosome-to-TGN pathway (Mallard et al., 1998; Mallard et al., 2002; Saint-Pol et al., 2004; Tai et al., 2004) but similar to that observed for STxB from detergent-soluble lipid microdomains of macrophages (Falguières et al., 2001) and for a subset of glycosphingolipids in fibroblasts from patients with sphingolipid-storage diseases (Marks and Pagano, 2002). One possibility, consistent with budding of tGolgin-1-enriched vesicles from Golgi membranes in vitro (Brown et al., 2001; Gleeson et al., 1996) and the apparent effect of a tGolgin-1 peptide on plasma-membrane accumulation of a glycosylphosphatidylinositol-linked marker (Kakinuma et al., 2004), is that tGolgin-1 participates in anterograde transport of a subset of cargo that might impact the overall cellular distribution of glycosphingolipids and/or cholesterol, as occurs in glycolipid-storage diseases (Marks and Pagano, 2002). Such a role for tGolgin-1 in anterograde transport might balance a retrograde pathway regulated by golgin-97 (Lu et al., 2004); interference with both pathways might restore the balance of lipids at the Golgi, potentially explaining why Golgi dispersal is not observed in cells depleted of Arl1 (Lu and Hong, 2003) or overproducing GRIP domains (Yoshino et al., 2003). Our studies thus provide a springboard for future investigations into the direct function of tGolgin-1 and the relationship between retrograde transport, lipid distribution and Golgi motility.

We thank C. Deutsch for help with statistical analyses, M. J. Birnbaum and H. Ohno for the use of their confocal microscopes, M. Lowe, B. Glick and J. Lippincott-Schwartz for gifts of plasmids encoding EGFP-tagged markers, H.-P. Hauri, and E. Berger for gifts of antibodies, and L. Ligon and M. Tokito for helpful discussions. This work was supported by the American Cancer Society (grant RPG-00-238-01-CSM to M.S.M.), NIH (grants R01 GM 048661 to E.L.H., R01 GM 061221 to C.G.B., and R01 GM 061012 to M.K.), l'Association pour la Recherche sur le Cancer (grants 5177 and 3105), Fondation de France – Programme Tumeurs (L.J.), and Post-doctoral Fellowship Award DAMD17-01-1-0365 from the US Army to A.Y.

References

Barr, F. A. (1999). A novel Rab6-interacting domain defines a family of Golgi-targeted coiled-coil proteins. *Curr. Biol.* **9**, 381-384.

Berger, E. G. and Hesford, F. J. (1985). Localization of galactosyl- and sialyltransferase by immunofluorescence: evidence for different sites. *Proc. Natl. Acad. Sci. USA* **82**, 4736-4739.

Bergmann, J. E., Tokuyasu, K. T. and Singer, S. J. (1981). Passage of an integral membrane protein, the vesicular stomatitis virus glycoprotein, through the Golgi apparatus en route to the plasma membrane. *Proc. Natl. Acad. Sci. USA* **78**, 1746-1750.

Berson, J. F., Theos, A. C., Harper, D. C., Tenza, D., Raposo, G. and Marks, M. S. (2003). Proprotein convertase cleavage liberates a fibrillogenic fragment of a resident glycoprotein to initiate melanosome biogenesis. *J. Cell Biol.* **161**, 521-533.

Bonifacino, J. S., Cosson, P. and Klausner, R. D. (1990). Colocalized transmembrane determinants for ER degradation and subunit assembly explain the intracellular fate of TCR chains. *Cell* **63**, 503-513.

Brown, D. L., Heimann, K., Lock, J., Kjer-Nielsen, L., van Vliet, C., Stow, J. L. and Gleeson, P. A. (2001). The GRIP domain is a specific targeting sequence for a population of trans-Golgi network derived tubulo-vesicular carriers. *Traffic* **2**, 336-344.

Brown, R. E. (1998). Sphingolipid organization in biomembranes: what physical studies of model membranes reveal. *J. Cell Sci.* **111**, 1-9.

Burkhardt, J. K., Echeverri, C. J., Nilsson, T. and Vallee, R. B. (1997). Overexpression of the dynamitin (p50) subunit of the dynactin complex disrupts dynein-dependent maintenance of membrane organelle distribution. *J. Cell Biol.* **139**, 469-484.

Cole, N. B., Sciaky, N., Marotta, A., Song, J. and Lippincott-Schwartz, J. (1996a). Golgi dispersal during microtubule disruption: regeneration of Golgi stacks at peripheral endoplasmic reticulum exit sites. *Mol. Biol. Cell* **7**, 631-650.

Cole, N. B., Smith, C. L., Sciaky, N., Terasaki, M., Edidin, M. and Lippincott-Schwartz, J. (1996b). Diffusional mobility of Golgi proteins in membranes of living cells. *Science* **273**, 797-801.

Corthesy-Theulaz, I., Pauloin, A. and Pfeffer, S. R. (1992). Cytoplasmic dynein participates in the centrosomal localization of the Golgi complex. *J. Cell Biol.* **118**, 1333-1345.

Cowan, D. A., Gay, D., Bieler, B. M., Zhao, H., Yoshino, A., Davis, J. G., Tomayko, M. M., Murali, R., Greene, M. I. and Marks, M. S. (2002). Characterization of mouse tGolgin-1 (golgin-245/ trans Golgi p230/ 256kD golgin) and its upregulation during oligodendrocyte development. *DNA Cell Biol.* **21**, 505-517.

Derby, M. C., van Vliet, C., Brown, D., Luke, M. R., Lu, L., Hong, W., Stow, J. L. and Gleeson, P. A. (2004). Mammalian GRIP domain proteins differ in their membrane binding properties and are recruited to distinct domains of the TGN. *J. Cell Sci.* **117**, 5865-5874.

Diao, A., Rahman, D., Pappin, D. J. C., Lucocq, J. and Lowe, M. (2003). The coiled-coil membrane protein golgin-84 is a novel Rab effector required for Golgi ribbon formation. *J. Cell Biol.* **160**, 201-212.

Elbashir, S. M., Harborth, J., Lendeckel, W., Yalcin, A., Weber, K. and Tuschl, T. (2001). Duplexes of 21-nucleotide RNAs mediate RNA interference in cultured mammalian cells. *Nature* **411**, 494-498.

Erlich, R., Gleeson, P. A., Campbell, P., Dietzsch, E. and Toh, B.-H. (1996). Molecular characterization of trans-Golgi p230. A human peripheral membrane protein encoded by a gene on chromosome 6p12-22 contains

extensive coiled-coil α-helical domains and a granin motif. *J. Biol. Chem.* **271**, 8328-8337.

Falguières, T., Mallard, F., Baron, C., Hanau, D., Lingwood, C., Goud, B., Salamero, J. and Johannes, L. (2001). Targeting of Shiga toxin B-subunit to retrograde transport route in association with detergent-resistant membranes. *Mol. Biol. Cell* **12**, 2453-2468.

Fritzler, M. J., Lung, C.-C., Hamel, J. C., Griffith, K. J. and Chan, E. K. L. (1995). Molecular characterization of golgin-245, a novel Golgi complex protein containing a granin signature. *J. Biol. Chem.* **270**, 31262-31268.

Ghosh, R. N., Mallet, W. G., Soe, T. T., McGraw, T. E. and Maxfield, F. R. (1998). An endocytosed TGN38 chimeric protein is delivered to the TGN after trafficking through the endocytic recycling compartment in CHO cells. *J. Cell Biol.* **142**, 923-936.

Gillingham, A. K., Tong, A. H. Y., Boone, C. and Munro, S. (2004). The GTPase Arf1p and the ER to Golgi cargo receptor Erv14p cooperate to recruit the golgin Rud3p to the cis-Golgi. *J. Cell Biol.* **167**, 281-292.

Gleeson, P. A., Anderson, T. J., Stow, J. L., Griffiths, G., Toh, B. H. and Matheson, F. (1996). p230 is associated with vesicles budding from the trans-Golgi network. *J. Cell Sci.* **109**, 2811-2821.

Griffith, K. J., Chan, E. K., Lung, C. C., Hamel, J. C., Guo, X., Miyachi, K. and Fritzler, M. J. (1997). Molecular cloning of a novel 97-kD Golgi complex autoantigen associated with Sjogren's syndrome. *Arthritis Rheum.* **40**, 1693-1702.

Hammond, A. T. and Glick, B. S. (2000). Dynamics of transitional endoplasmic reticulum sites in vertebrate cells. *Mol. Biol. Cell* **11**, 3013-3030.

Harada, A., Takei, Y., Kanai, Y., Tanaka, Y., Nonaka, S. and Hirokawa, N. (1998). Golgi vesiculation and lysosome dispersion in cells lacking cytoplasmic dynein. *J. Cell Biol.* **141**, 51-59.

Ho, W. C., Allan, V. J., van Meer, G., Berger, E. G. and Kreis, T. E. (1989). Reclustering of scattered Golgi elements occurs along microtubules. *Eur. J. Cell Biol.* **48**, 250-263.

Holleran, E. A., Ligon, L. A., Tokito, M., Stankewich, M. C., Morrow, J. S. and Holzbaur, E. L. F. (2001). βIII spectrin binds to the Arp1 subunit of dynactin. *J. Biol. Chem.* **276**, 36598-36605.

Infante, C., Ramos-Morales, F., Fedriani, C., Bornens, M. and Rios, R. M. (1999). GMAP-210, a cis-Golgi network-associated protein, is a minus end microtubule-binding protein. *J. Cell Biol.* **145**, 83-98.

Johannes, L. and Goud, B. (1998). Surfing on a retrograde wave: how does Shiga toxin reach the endoplasmic reticulum? *Trends Cell Biol.* **8**, 158-162.

Kakinuma, T., Ichikawa, H., Tsukada, Y., Nakamura, T. and Toh, B. H. (2004). Interaction between p230 and MACF1 is associated with transport of a glycosyl phosphatidyl inositol-anchored protein from the Golgi to the cell periphery. *Exp. Cell Res.* **298**, 388-398.

Kjer-Nielsen, L., Teasdale, R. D., van Vliet, C. and Gleeson, P. A. (1999a). A novel Golgi-localisation domain shared by a class of coiled-coil peripheral membrane proteins. *Curr. Biol.* **9**, 385-388.

Kjer-Nielsen, L., van Vliet, C., Erlich, R., Toh, B.-H. and Gleeson, P. A. (1999b). The Golgi targeting sequence of the peripheral membrane protein p230. *J. Cell Sci.* **112**, 1645-1654.

Ladinsky, M. S., Mastronarde, D. N., McIntosh, J. R., Howell, K. E. and Staehelin, L. A. (1999). Golgi structure in three dimensions: functional insights from the Normal Rat Kidney cell. *J. Cell Biol.* **144**, 1135-1149.

Lane, J. D., Lucocq, J., Pryde, J., Barr, F. A., Woodman, P. G., Allan, V. J. and Lowe, M. (2002). Caspase-mediated cleavage of the stacking protein GRASP65 is required for Golgi fragmentation during apoptosis. *J. Cell Biol.* **156**, 495-509.

Li, B. and Warner, J. R. (1996). Mutation of the Rab6 homologue of *Saccharomyces cerevisiae*, YPT6, inhibits both early Golgi function and ribosome biosynthesis. *J. Biol. Chem.* **271**, 16813-16819.

Linstedt, A. D. and Hauri, H. P. (1993). Giantin, a novel conserved Golgi membrane protein containing a cytoplasmic domain of at least 350 kDa. *Mol. Biol. Cell* **4**, 679-693.

Lu, L. and Hong, W. (2003). Interaction of Arl1-GTP with GRIP domains recruits autoantigens Golgin-97 and golgin-245/p230 onto the Golgi. *Mol. Biol. Cell* **14**, 3767-3781.

Lu, L., Tai, G. and Hong, W. (2004). Autoantigen golgin-97, an effector of Arl1 GTPase, participates in traffic from the endosome to the TGN. *Mol. Biol. Cell* **15**, 4426-4443.

Luke, M. R., Kjer-Nielsen, L., Brown, D. L., Stow, J. L. and Gleeson, P. A. (2003). GRIP domain-mediated targeting of two new coiled coil proteins, GCC88 and GCC185, to subcompartments of the trans-Golgi network. *J. Biol. Chem.* **278**, 4216-4226.

Mallard, F., Antony, C., Tenza, D., Salamero, J., Goud, B. and Johannes, L. (1998). Direct pathway from early/recycling endosomes to the Golgi apparatus revealed through the study of Shiga toxin B-fragment transport. *J. Cell Biol.* **143**, 973-990.

Mallard, F., Tang, B. L., Galli, T., Tenza, D., Saint-Pol, A., Yue, X., Antony, C., Hong, W., Goud, B. and Johannes, L. (2002). Early/recycling endosomes-to-TGN transport involves two SNARE complexes and a Rab6 isoform. *J. Cell Biol.* **156**, 653-664.

Mallet, W. G. and Maxfield, F. R. (1999). Chimeric forms of furin and TGN38 are transported with the plasma membrane in the trans-Golgi network via distinct endosomal pathways. *J. Cell Biol.* **146**, 345-359.

Malsam, J., Satoh, A., Pelletier, L. and Warren, G. (2005). Golgin tethers define subpopulations of COPI vesicles. *Science* **307**, 1095-1098.

Marks, D. L. and Pagano, R. E. (2002). Endocytosis and sorting of glycosphingolipids in sphingolipid storage disease. *Trends Cell Biol.* **12**, 605-613.

Marks, M. S., Roche, P. A., van Donselaar, E., Woodruff, L., Peters, P. J. and Bonifacino, J. S. (1995). A lysosomal targeting signal in the cytoplasmic tail of the β chain directs HLA-DM to the MHC class II compartments. *J. Cell Biol.* **131**, 351-369.

Marks, M. S., Woodruff, L., Ohno, H. and Bonifacino, J. S. (1996). Protein targeting by tyrosine- and di-leucine-based signals: evidence for distinct saturable components. *J. Cell Biol.* **135**, 341-354.

Marsh, B. J., Mastronarde, D. N., Buttle, K. F., Howell, K. E. and McIntosh, R. J. (2001). Organellar relationships in the Golgi region of the pancreatic beta cell line, HIT-T15, visualized by high resolution electron tomography. *Proc. Natl. Acad. Sci. USA* **98**, 2399-2406.

Matanis, T., Akhmanova, A., Wulf, P., del Nery, E., Weide, T., Stepanova, T., Galjart, N., Grosveld, F., Goud, B., de Zeeuw, C. I. et al. (2002). Bicaudal-D regulates COPI-independent Golgi-ER transport by recruiting the dynein-dynactin motor complex. *Nat. Cell Biol.* **4**, 986-992.

McCaffery, J. M. and Farquhar, M. G. (1995). Localization of GTPases (GTP-binding proteins) by indirect immunofluorescence and immunoelectron microscopy. *Methods Enzymol.* **257**, 259-279.

Munro, S. and Nichols, B. J. (1999). The GRIP domain – a novel Golgi-targeting domain found in several coiled-coil proteins. *Curr. Biol.* **9**, 377-380.

Muresan, V., Stankewich, M. C., Steffen, W., Morrow, J. S., Holzbaur, E. L. and Schnapp, B. J. (2001). Dynactin-dependent, dynein-driven vesicle transport in the absence of membrane proteins: a role for spectrin and acidic phospholipids. *Mol. Cell* **7**, 173-183.

Natarajan, R. and Linstedt, A. D. (2004). A cycling cis Golgi protein mediates endosome-to-Golgi traffic. *Mol. Biol. Cell* **15**, 4798-4806.

Panic, B., Perisic, O., Veprintsev, D. B., Williams, R. L. and Munro, S. (2003a). Structural basis for Arl1-dependent targeting of homodimeric GRIP domains to the Golgi apparatus. *Mol. Cell* **12**, 863-874.

Panic, B., Whyte, J. R. C. and Munro, S. (2003b). The Arf-like GTPases Arl1p and Arl3p act in a pathway that interacts with vesicle-tethering factors at the Golgi apparatus. *Curr. Biol.* **13**, 405-410.

Perez, F., Pernet-Gallay, K., Nizak, C., Goodson, H. V., Kreis, T. E. and Goud, B. (2002). CLIPR-59, a new trans-Golgi/TGN cytoplasmic linker protein belonging to the CLIP-170 family. *J. Cell Biol.* **156**, 631-642.

Pernet-Gallay, K., Antony, C., Johannes, L., Bornens, M., Goud, B. and Rios, R. M. (2002). The overexpression of GMAP-210 blocks anterograde and retrograde transport between the ER and the Golgi apparatus. *Traffic* **3**, 822-832.

Presley, J. F., Cole, N. B., Schroer, T. A., Hirschberg, K., Zaal, K. J. M. and Lippincott-Schwartz, J. (1997). ER-to-Golgi transport visualized in living cells. *Nature* **389**, 81-85.

Reaves, B. and Banting, G. (1992). Perturbation of the morphology of the trans-Golgi network following brefeldin A treatment: redistribution of a TGN-specific integral membrane protein, TGN38. *J. Cell Biol.* **116**, 85-94.

Rios, R. M. and Bornens, M. (2003). The Golgi apparatus at the cell centre. *Curr. Opin. Cell Biol.* **15**, 60-66.

Rios, R. M., Sanchis, A., Tassin, A. M., Fedriani, C. and Bornens, M. (2004). GMAP-210 recruits γ-tubulin complexes to cis-Golgi membranes and is required for Golgi ribbon formation. *Cell* **118**, 323-335.

Rogalski, A. A. and Singer, S. J. (1984). Associations of elements of the Golgi apparatus with microtubules. *J. Cell Biol.* **99**, 1092-1100.

Saint-Pol, A., Yélamos, B., Amessou, M., Mills, I., Dugast, M., Tenza, D., Schu, P., Antony, C., McMahon, H. T., Lamaze, C. et al. (2004). Clathrin adaptor epsinR is required for retrograde sorting on early endosomal membranes. *Dev. Cell* **6**, 532-538.

Sandvig, K. and van Deurs, B. (2002). Transport of protein toxins into cells: pathways used by ricin, cholera toxin and Shiga toxin. *FEBS Lett.* **529**, 49-53.

Santini, F., Marks, M. S. and Keen, J. H. (1998). Endocytic clathrin-coated pit formation is independent of receptor internalization signal levels. *Mol. Biol. Cell* **9**, 1177-1194.

Seaman, M. N. (2004). Cargo-selective endosomal sorting for retrieval to the Golgi requires retromer. *J. Cell Biol.* **165**, 111-122.

Setty, S. R. G., Shin, M. E., Yoshino, A., Marks, M. S. and Burd, C. G. (2003). Golgi recruitment of GRIP domain proteins by ARF-like GTPase 1 (Arl1p) is regulated by Arf-like GTPase 3 (Arl3p). *Curr. Biol.* **13**, 401-404.

Short, B., Preisinger, C., Schaletzky, J., Kopajtich, R. and Barr, F. A. (2002). The Rab6 GTPase regulates recruitment of the dynactin complex to Golgi membranes. *Curr. Biol.* **12**, 1792-1795.

Siniossoglou, S., Peak-Chew, S. Y. and Pelham, H. R. B. (2000). Ric1p and Rgp1p form a complex that catalyses nucleotide exchange on Ypt6p. *EMBO J.* **19**, 4885-4894.

Sprong, H., Degroote, S., Claessens, T., van Drunen, J., Oorschot, V., Westerink, B. H. C., Hirabayashi, Y., Klumperman, J., van der Sluijs, P. and van Meer, G. (2001). Glycosphingolipids are required for sorting melanosomal proteins in the Golgi complex. *J. Cell Biol.* **155**, 369-380.

Storrie, B., White, J., Röttger, S., Stelzer, E. H. K., Suganuma, T. and Nilsson, T. (1998). Recycling of Golgi-resident glycosyltransferases through the ER reveals a novel pathway and provides an explanation for nocodazole-induced Golgi scattering. *J. Cell Biol.* **143**, 1505-1521.

Stüven, E., Porat, A., Shimron, F., Fass, E., Kaloyanova, D., Brügger, B., Wieland, F. T., Elazar, Z. and Helms, J. B. (2003). Intra-Golgi protein transport depends on a cholesterol balance in the lipid membrane. *J. Biol. Chem.* **278**, 53112-53122.

Tai, G., Lu, L., Wang, T. L., Tang, B. L., Goud, B., Johannes, L. and Hong, W. (2004). Participation of the syntaxin 5/Ykt6/GS28/GS15 SNARE complex in transport from the early/recycling endosome to the TGN. *Mol. Biol. Cell* **15**, 4011-4022.

Takahashi, M., Shibata, H., Shimakawa, M., Miyamoto, M., Mukai, H. and Ono, Y. (1999). Characterization of a novel giant scaffolding protein, CG-NAP, that anchors multiple signaling enzymes to centrosome and the Golgi apparatus. *J. Biol. Chem.* **274**, 17267-17274.

Tsukada, M., Will, E. and Gallwitz, D. (1999). Structural and functional analysis of a novel coiled-coil protein involved in Ypt6 GTPase-regulated protein transport in yeast. *Mol. Biol. Cell* **10**, 63-75.

van Meer, G. (2002). Cell biology. The different hues of lipid rafts. *Science* **296**, 855-857.

Wagner, M., Rajasekaran, A. K., Hanzel, D. K., Mayor, S. and Rodriguez-Boulan, E. (1994). Brefeldin A causes structural and functional alterations of the trans-Golgi network of MDCK cells. *J. Cell Sci.* **107**, 933-943.

Walenta, J. H., Didier, A. J., Liu, X. and Kramer, H. (2001). The Golgi-associated Hook3 protein is a member of a novel family of microtubule-binding proteins. *J. Cell Biol.* **152**, 923-934.

Warren, G. and Shorter, J. (2002). Golgi architecture and inheritance. *Annu. Rev. Cell Dev. Biol.* **18**, 379-420.

Whiteman, E. L., Chen, J. J. and Birnbaum, M. J. (2003). Platelet-derived growth factor (PDGF) stimulates glucose transport in 3T3-L1 adipocytes overexpressing PDGF receptor by a pathway independent of insulin receptor substrates. *Endocrinology* **144**, 3811-3820.

Wu, M., Lu, L., Hong, W. and Song, H. (2004). Structural basis for recruitment of GRIP domain golgin-245 by small GTPase Arl1. *Nat. Struct. Mol. Biol.* **11**, 86-94.

Wu, X., Rao, K., Bowers, M. B., Copeland, N. G., Jenkins, N. A. and Hammer, J. A. (2001). Rab27a enables myosin Va-dependent melanosome capture by recruiting the myosin to the organelle. *J. Cell Sci.* **114**, 1091-1100.

Xu, Y., Takeda, S., Nakata, T., Noda, Y., Tanaka, Y. and Hirokawa, N. (2002). Role of KIFC3 motor protein in Golgi positioning and integration. *J. Cell Biol.* **158**, 293-303.

Yoshino, A., Bieler, B. M., Harper, D. C., Cowan, D. A., Sutterwala, S., Gay, D. M., Cole, N. B., McCaffery, J. M. and Marks, M. S. (2003). A role for GRIP domain proteins and/or their ligands in structure and function of the trans Golgi network. *J. Cell Sci.* **116**, 4441-4454.